Lecture 12 Powder Diffraction

Synchrotron powder diffraction for structural materials science

Eiji Nishibori

Department of Applied Physics, Nagoya University, Nagoya, Japan

eiji@mcr.nuap.nagoya-u.ac.jp

SESAME-KEK School 2011

Materials Science

Materials science is an interdisciplinary field involving the properties of matter and its applications to various areas of science.
Materials science investigates the relationship between the structure of materials and their macroscopic properties.

Materials Science

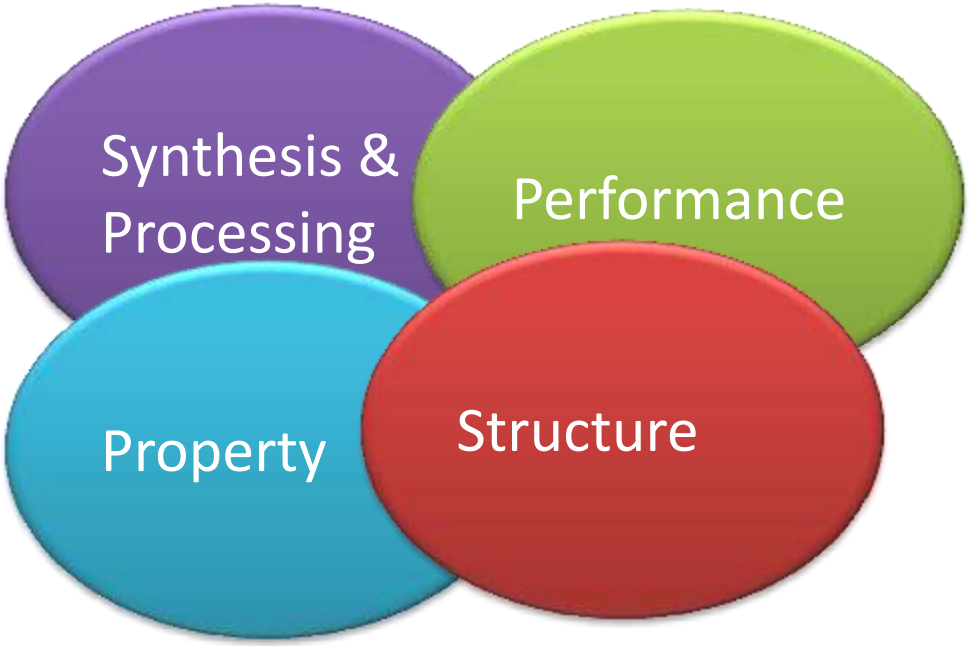

X-ray diffraction crystallography is a method of determining the structure.

Target Materials.

- Macromolecule,
- Organic molecule,
- Inorganic materials etc,

X-ray diffraction techniques

- Single-crystal X-ray diffraction
- **Powder diffraction**
- Thin film & fiber diffraction

Powder Diffraction

Laboratory Diffractometer

Electronics
- Condenser
- piezoelectric materials
- semiconductor etc.

Thermoelectric materials

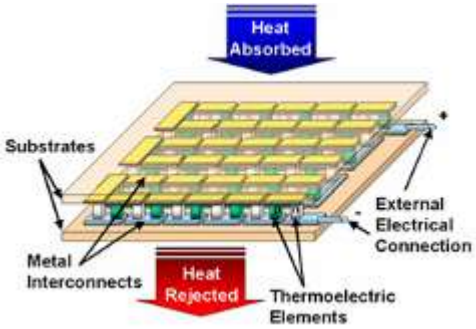

Powder diffraction is an indispensable technique for materials characterization of relatively simple inorganic materials widely used in laboratories.

- Phase identification
- Qualitative structure analysis,
- Measurements of lattice parameters,
- Estimation of crystallinity, etc.

The great advantages of the powder diffraction technique:

- Simplicity of sample preparation

  Many materials are readily available for powder diffraction

- Rapidity of measurement

  Collection times can be quite short, since all possible crystal orientations are measured simultaneously

Powder diffraction is one of the most powerful methods to identify and characterize new materials

Target materials for SR powder diffraction

Protein

Semiconductor

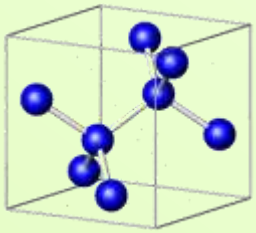

Acta Cryst. A. 2007

Thermoelectrics

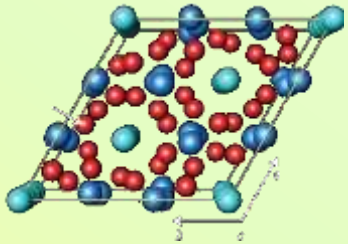

Nature Materials 2004
Phys. Rev. B. 2007

Pharmaceuticals

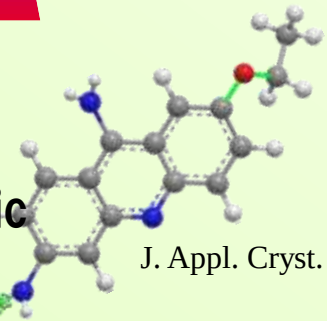

J. Appl. Cryst. 2008

Superconductor

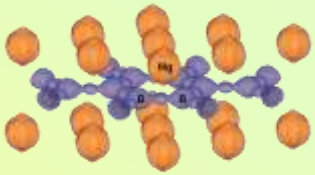

JPSJ. 2001

Nano-carbon materiials

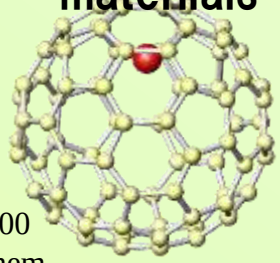

Nature. 2000
Angew. Chem. 2000,2005

Metal organic materials.

Angew. Chem. 2006

Chemistry, Materials Scinece

SR Powder diffraction can apply wide variety of materials

Contents

- Principle of Powder Diffraction.
- Advantages of SR powder diffraction.
- Analytical technique of powder data.
- Structural studies of SR powder diffraction

X-ray Diffraction from single crystal

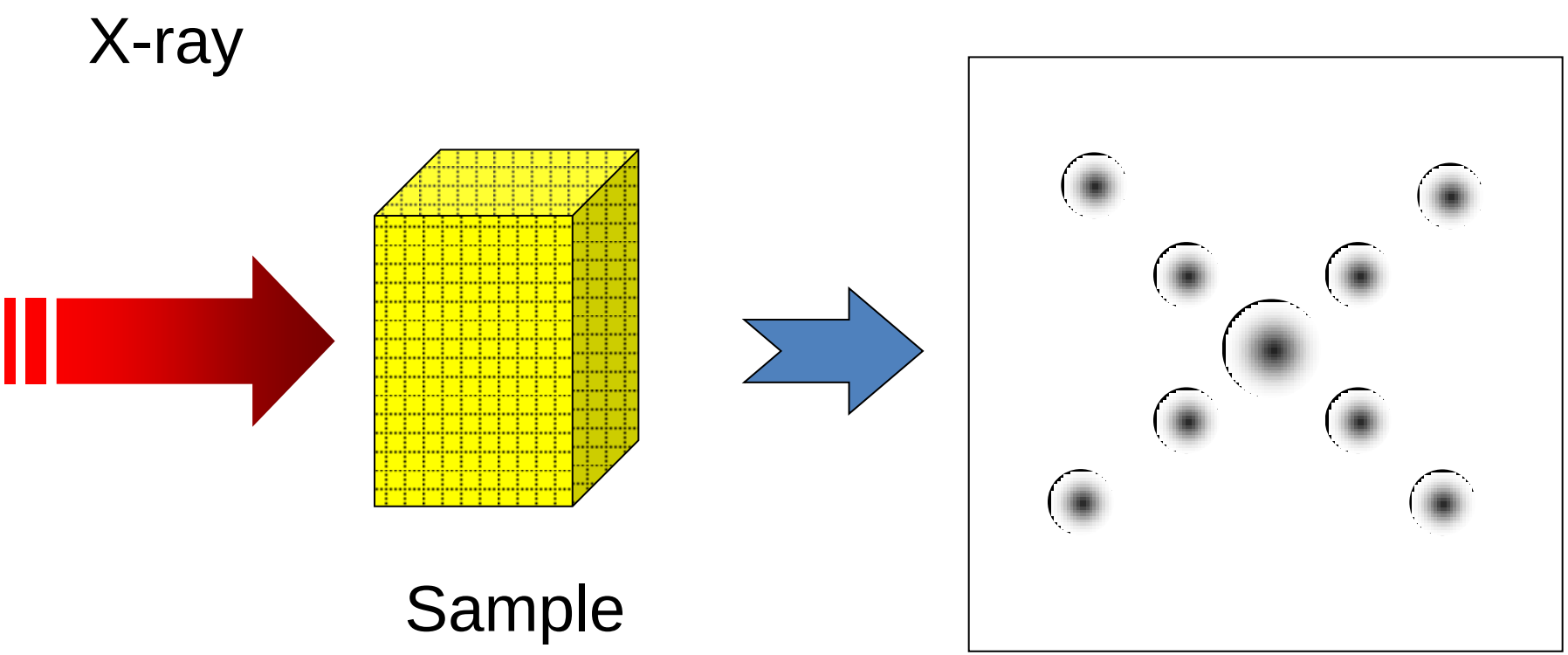

The incident beam coming from left causes scatter.

Part of the incident beam is deflected, producing a reflection spot in the diffraction pattern like this.

X-ray Diffraction from powder crystal

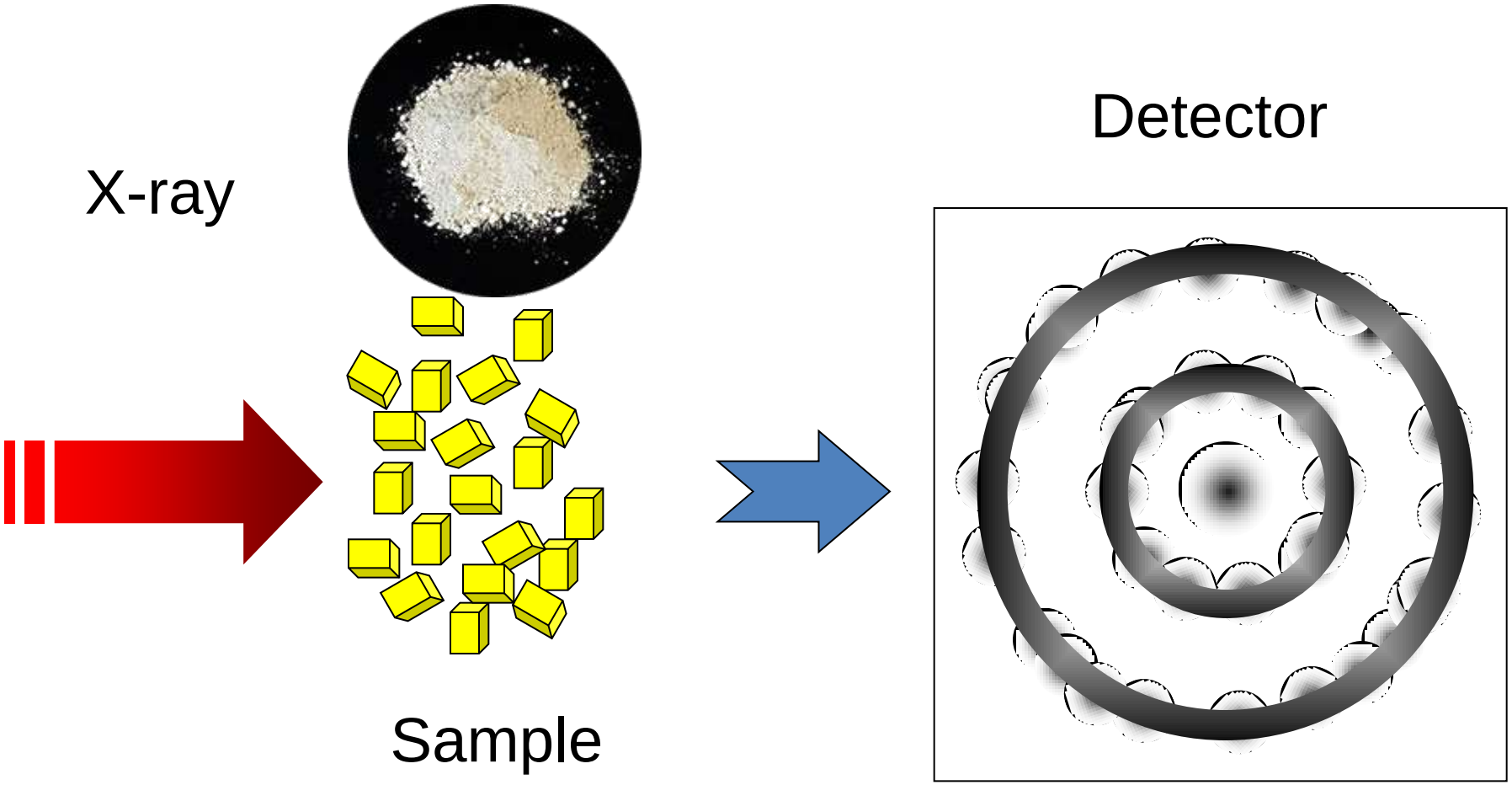

aggregate of small single crystals

Crystals which satisfy the Bragg's reflection condition can reflect X-ray beam.

A set of diffracting beams from crystal planes makes a ring.

Powder diffraction data.

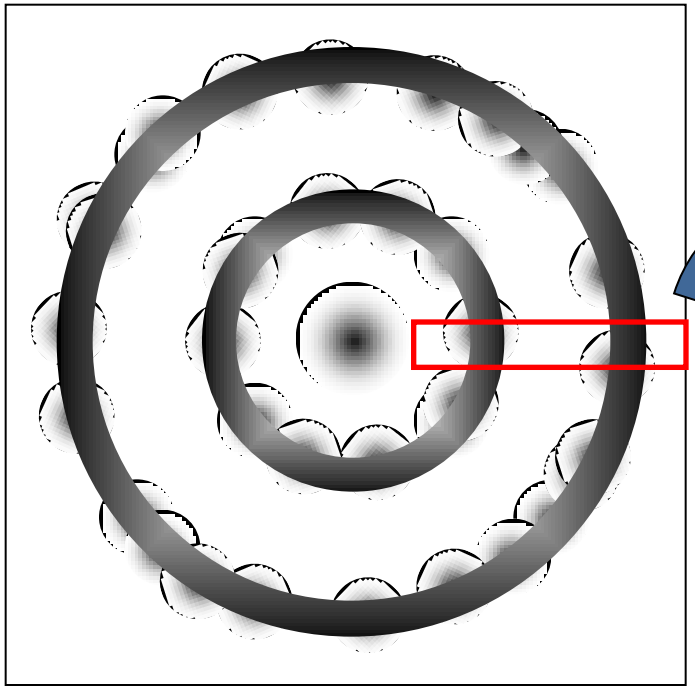

Many rings, actually cones, of diffracted beam are created.

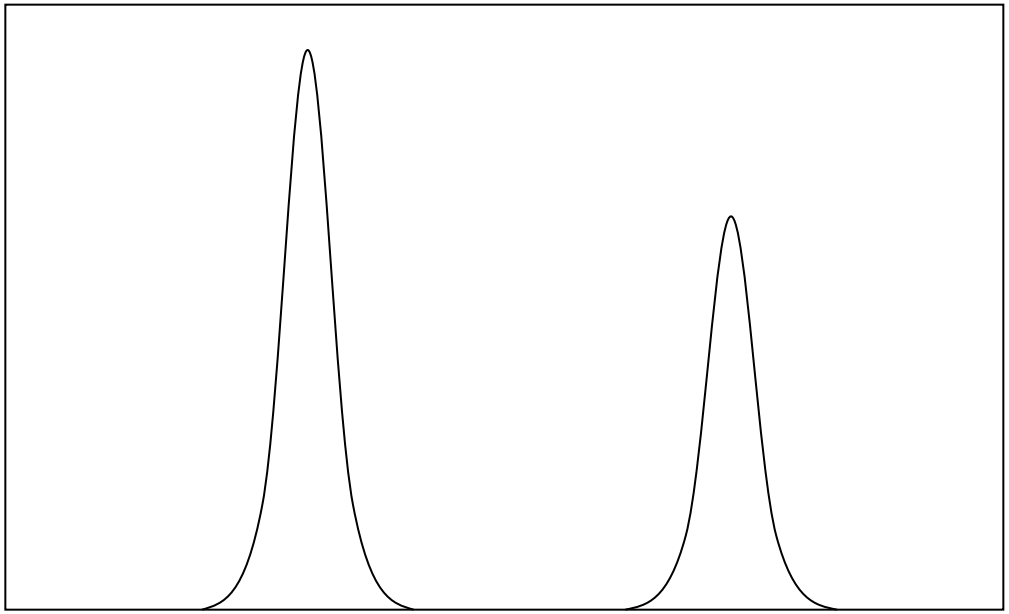

2θ

If a beam hits a powder sample, we can easily observe a diffraction pattern by scanning along this line.

The disadvantages of the powder diffraction technique:

- Difficult to measure each individual Bragg intensity due to peak overlap

  Many information is lost by the collapse of the 3D space onto a 1D axis.
- Difficult to measure weak Bragg intensities

  such as super lattice & forbidden reflections, reflection in high angle region

Structure determination and Accurate structural analysis from powder diffraction is normally difficult.

Peak Overlap

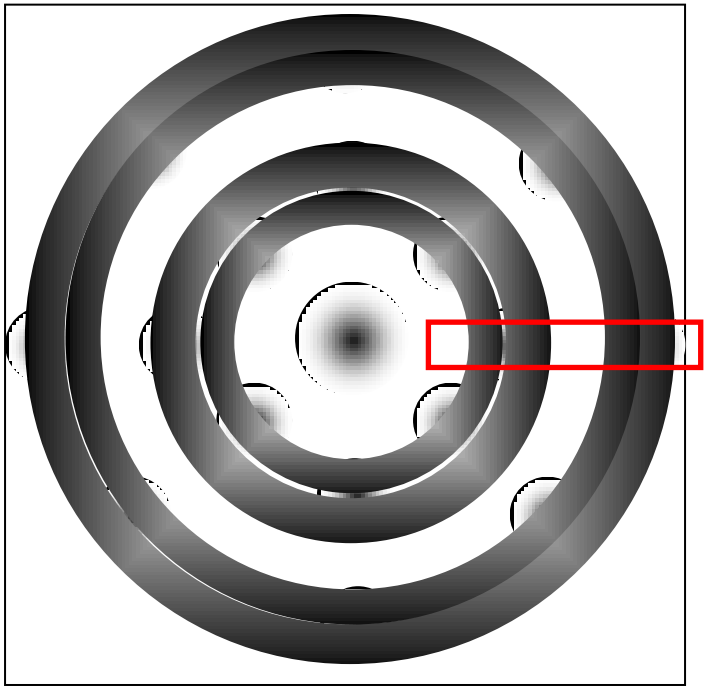

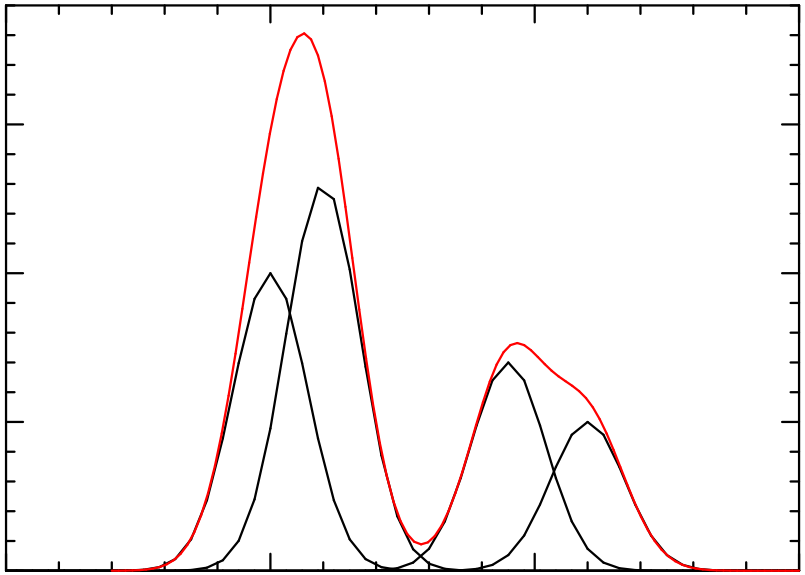

2θ

Peaks are overlapped.

This is unavoidable and essential disadvantage of powder diffraction.

Intensity from crystal

Unit cell

$\vec{a},\vec{b},\vec{c}$ Lattice vector

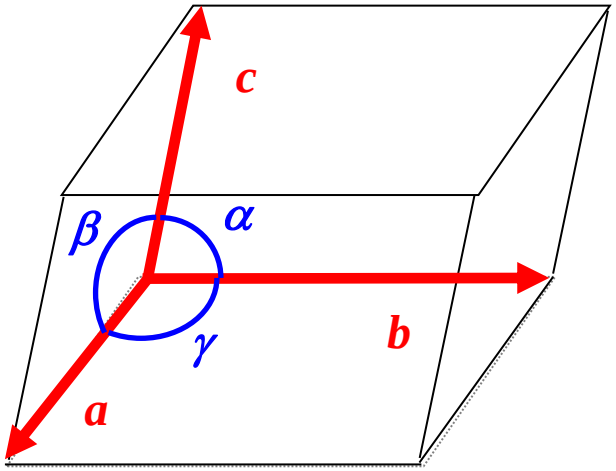

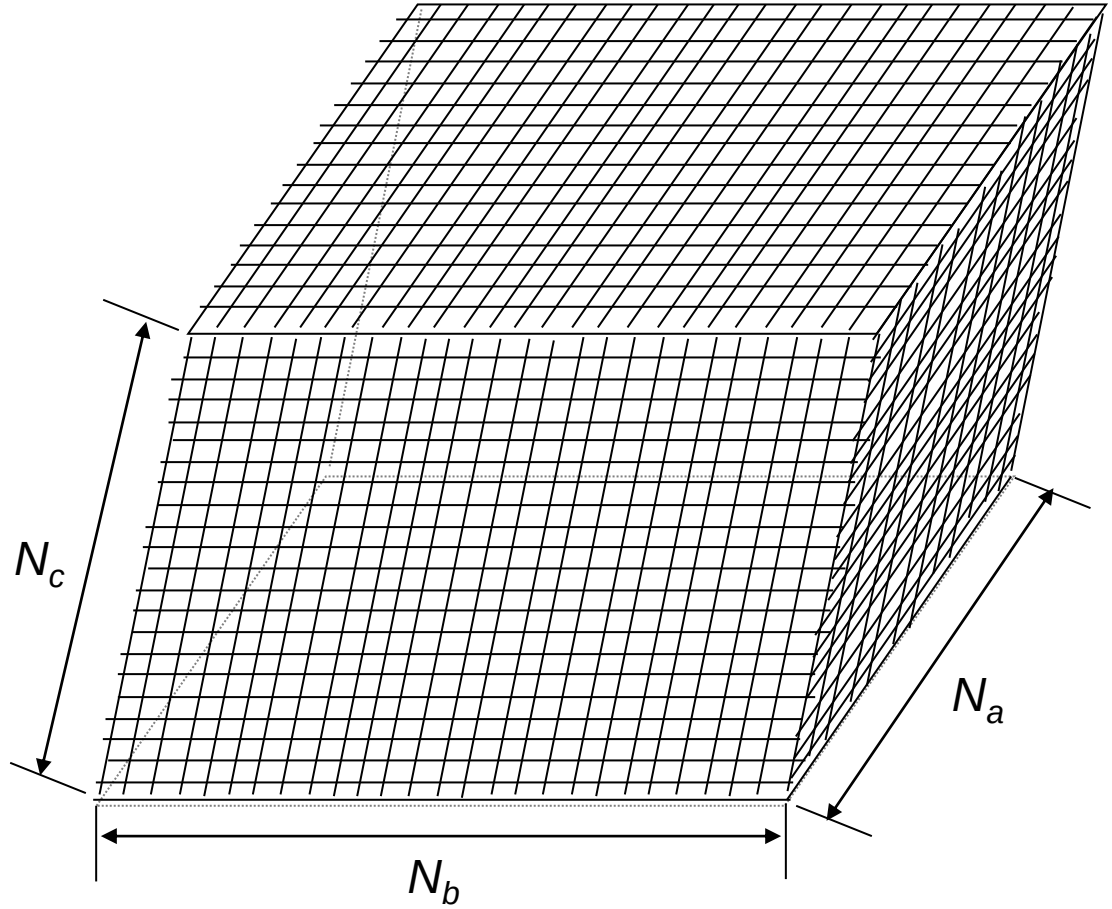

$$I_{Wholecrystal} \propto \left| \sum_{h=0}^{N_a-1} \sum_{k=0}^{N_b-1} \sum_{l=0}^{N_c-1} \exp\left(2\pi i \vec{K} \cdot \left(h\vec{a} + k\vec{b} + l\vec{c}\right)\right) F\left(\vec{K}\right) \right|^2$$

$$\left| \sum_{h=0}^{N_a-1} \sum_{k=0}^{N_b-1} \sum_{l=0}^{N_c-1} exp\left(2\pi i \vec{K} \cdot \left(h\vec{a} + k\vec{b} + l\vec{c}\right)\right) \right|^2 = \frac{sin^2\left(2\pi \vec{K} \cdot N_a a\right)}{sin^2\left(2\pi \vec{K} \cdot a\right)} \frac{sin^2\left(2\pi \vec{K} \cdot N_b b\right)}{sin^2\left(2\pi \vec{K} \cdot b\right)} \frac{sin^2\left(2\pi \vec{K} \cdot N_c c\right)}{sin^2\left(2\pi \vec{K} \cdot c\right)}$$

Intensity from crystal

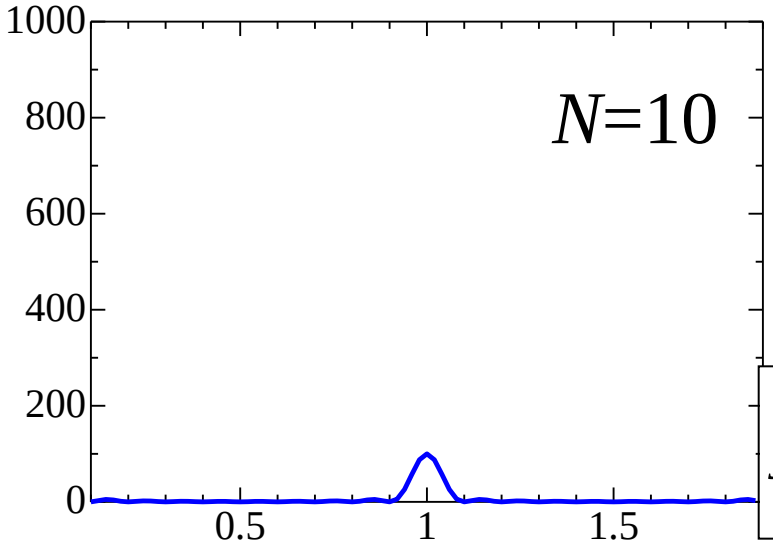

$$y = \frac{\sin^2\left(2\pi\vec{K}\cdot Na\right)}{\sin^2\left(2\pi\vec{K}\cdot a\right)}$$

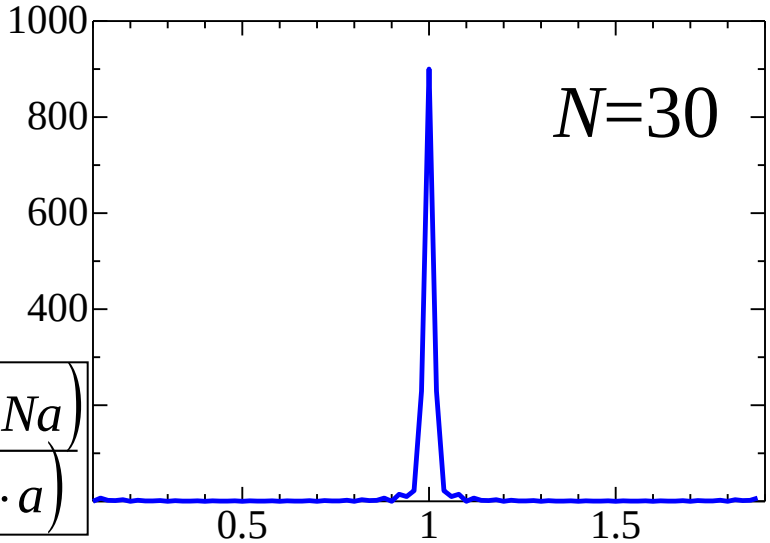

An Intensity from a crystal proportional to square of the total number of unit cell in the crystal.

$$I_{Whole crystal} \propto N^2 \left| F\left(\vec{K}\right)\right|^2$$

Typical size of sample

Single Crystal : ~100μm

Powder Crystal : ~1μm

An Intensity from 1μm powder crystal is much smaller, $1/((100)^3)^2$, than that from 100μm single crystal. Intensity of powder diffraction is much weaker than single crystal diffraction.

Powder data of novel nano-materials measured at Lab X-ray Source.

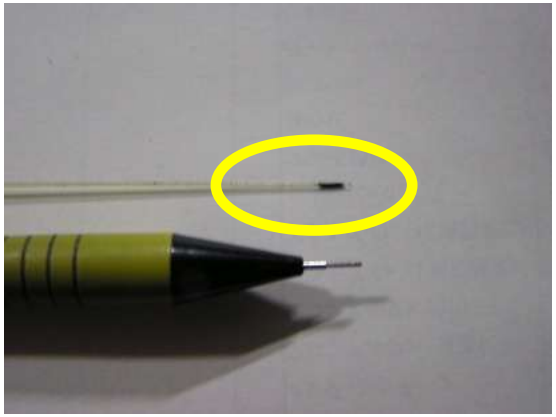

Endohedral Metallofullerene

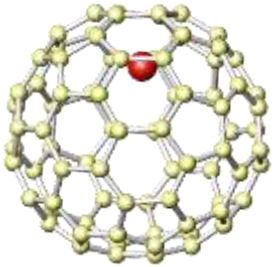

Newly synthesized nano-structured materials are usually obtained in powder form.

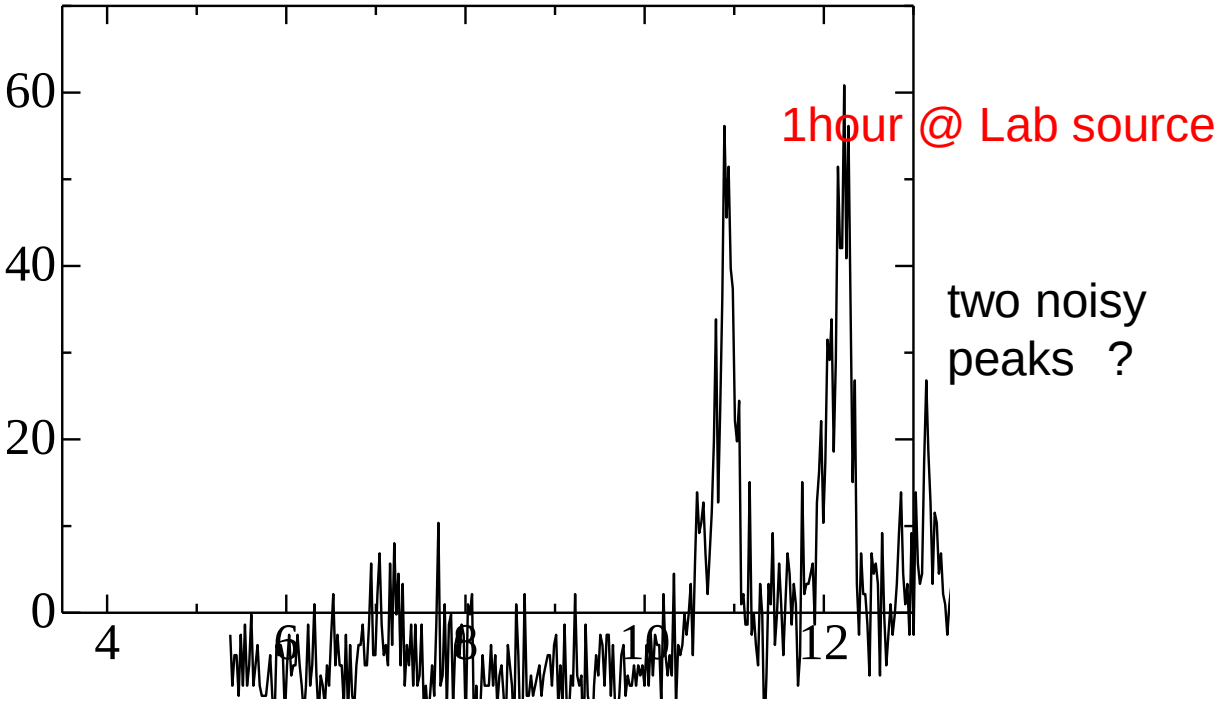

It is almost impossible to determine the structure from this data.

Advantages of SR powder Diffraction.

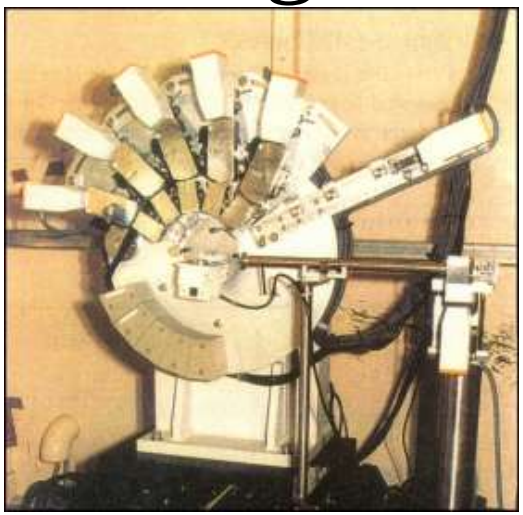

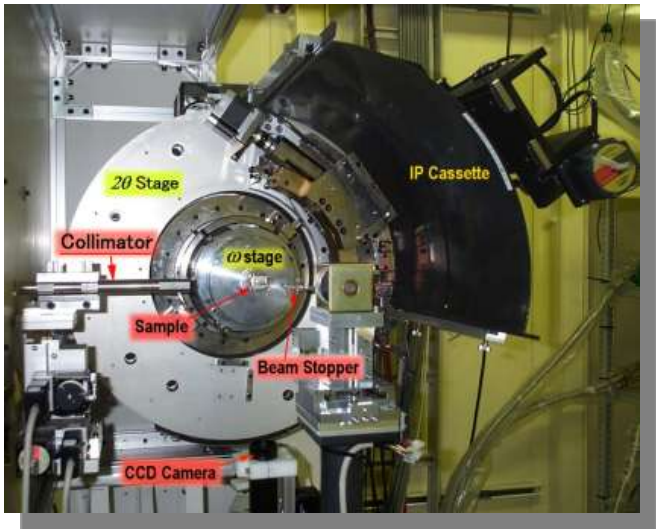

An X-ray at SR source has great advantages for powder diffraction study. X-ray beam with high-energy resolution and sufficiently high-intensity is available.

High quality powder diffraction data

SR powder diffractometers at Japanese synchrotron facilities

Multiple detector system(MDS) at Photon Factory

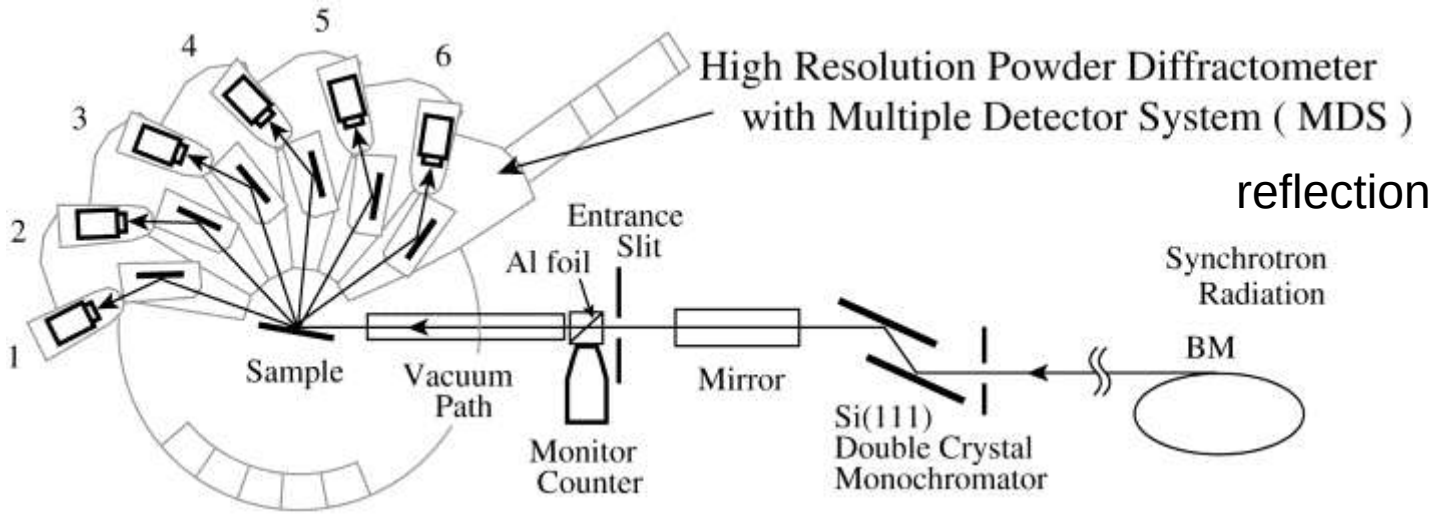

reflection geometry

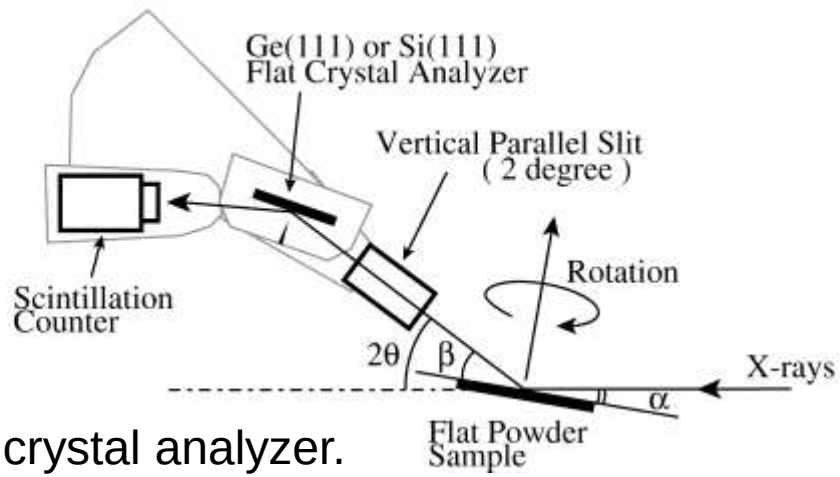

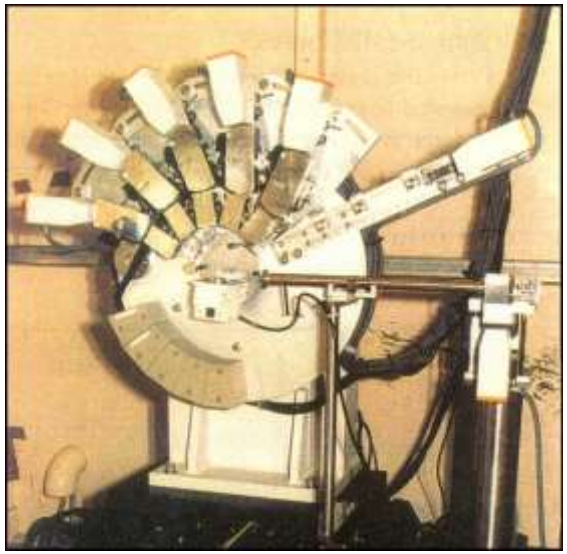

Each arm has crystal analyzer.

In the measurement by step scan, it takes much time because of the small step angle. But MDS enables us to measure within rather short time by multiple detectors.

Parts of diffraction patterns of Mg2SiO4

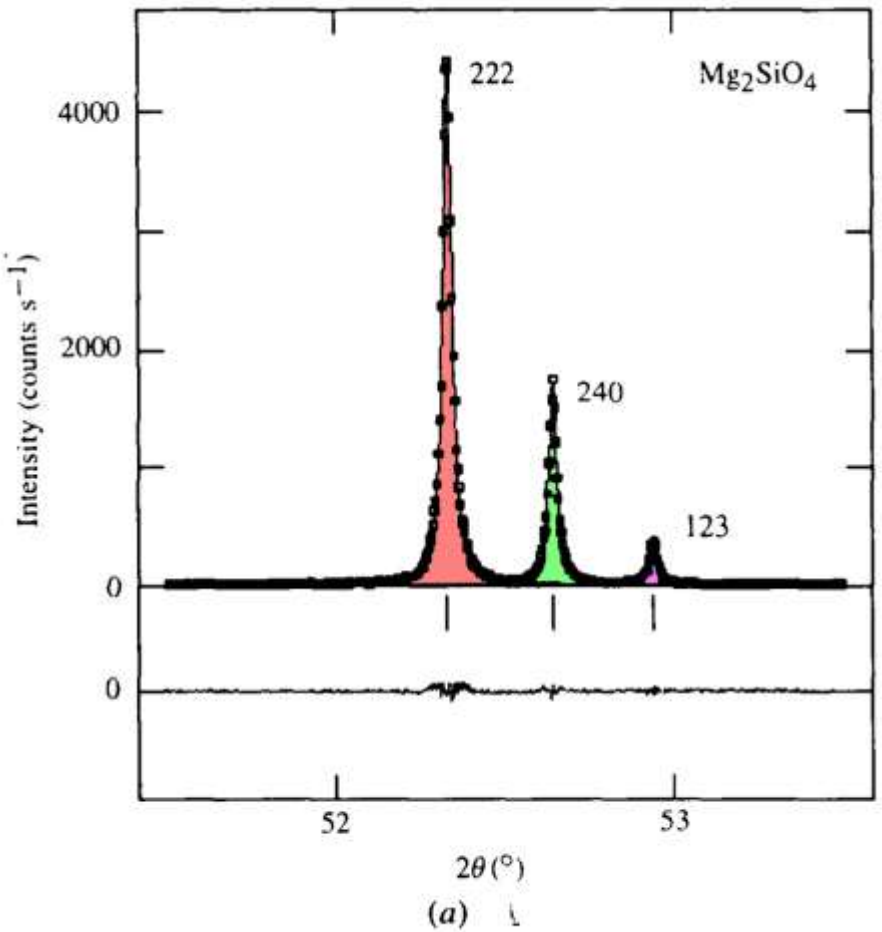

(a) MDS

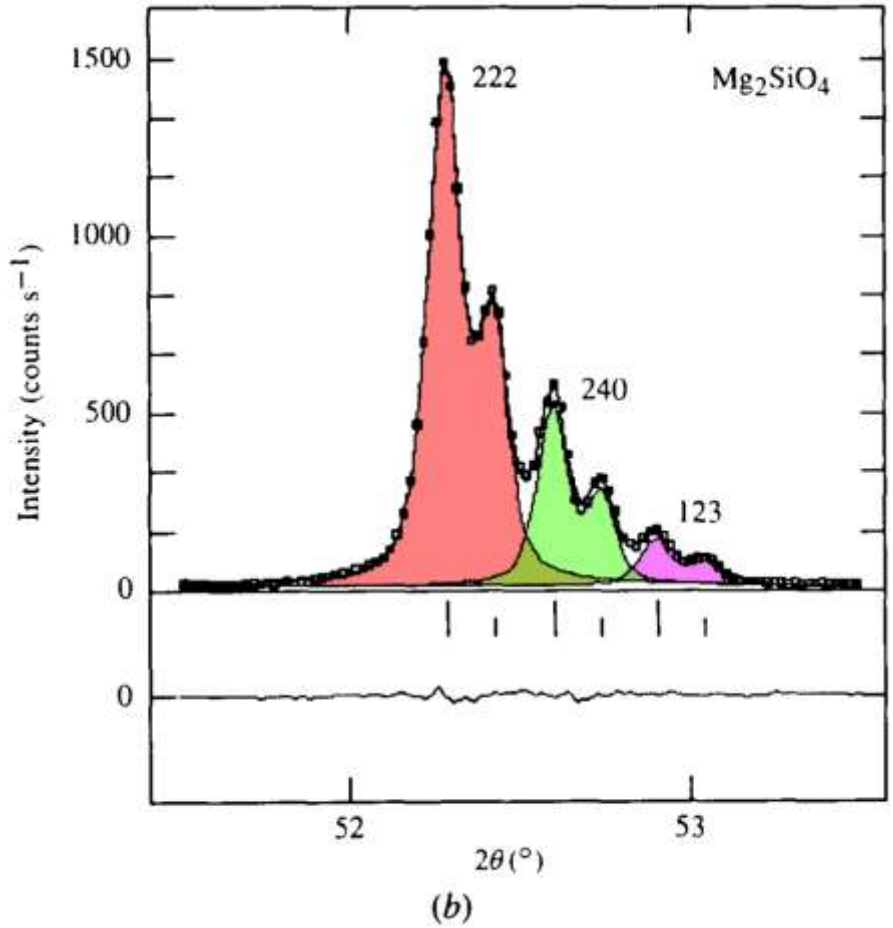

(b) ordinary-type diffractometer using lab source.

A comparison of three overlapping reflections from Mg2SiO4 , showing a well resolved pattern for the MDS.

Large Debye-Scherrer camera at SPring-8 BL02B2

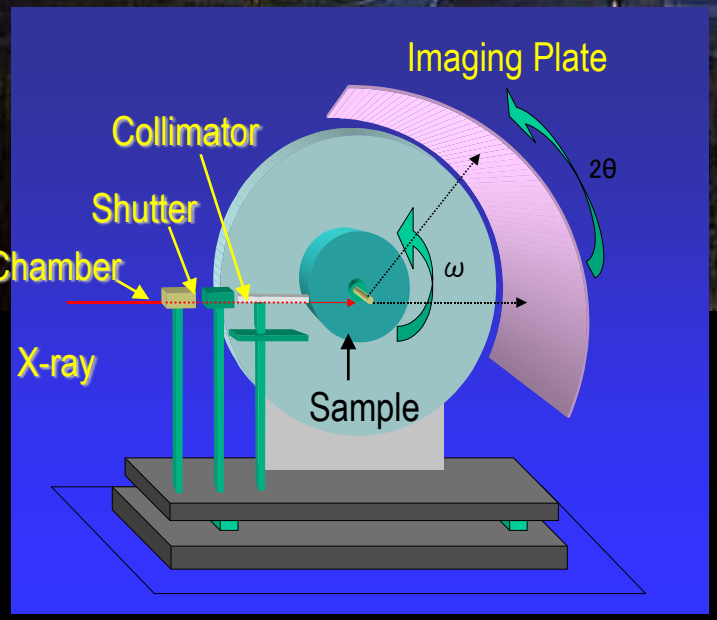

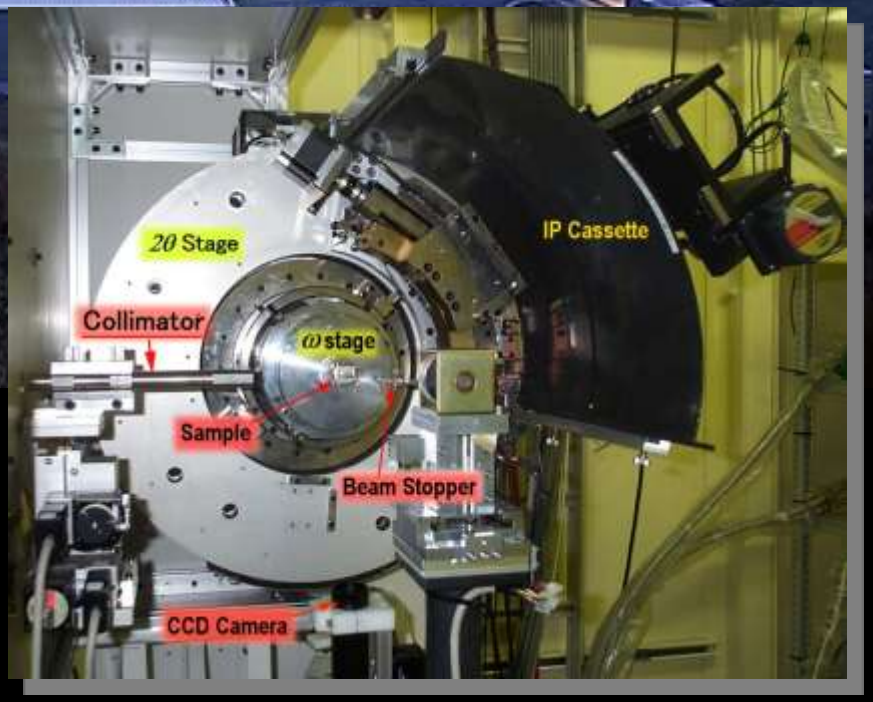

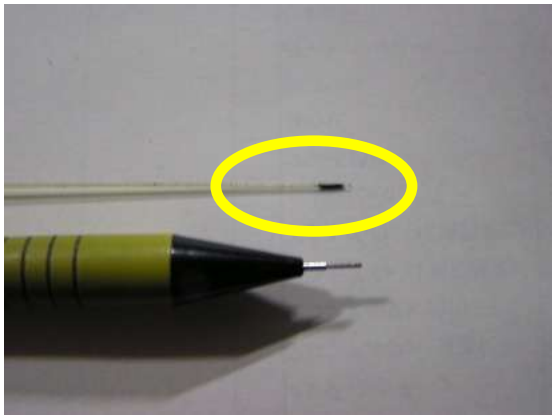

Endohedral Metallofullerene

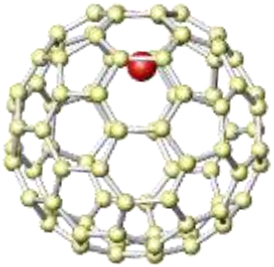

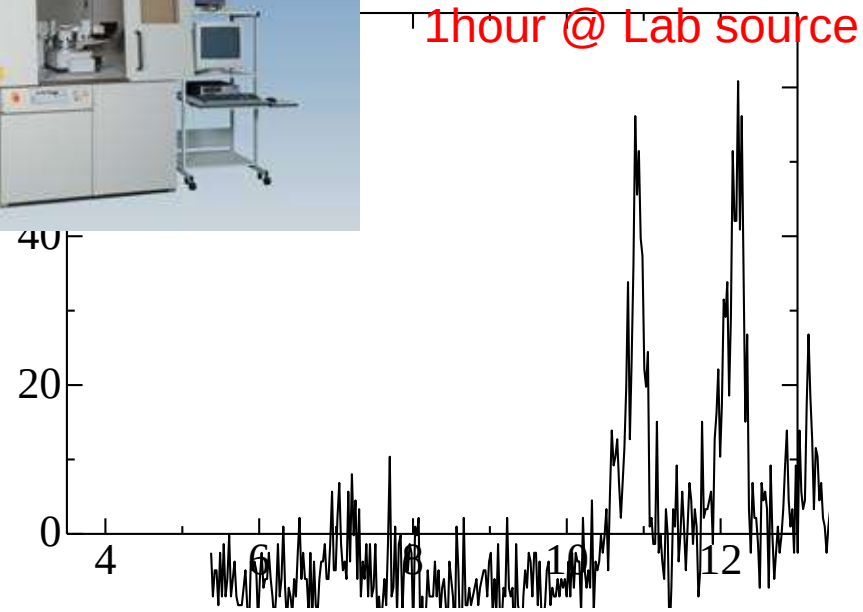

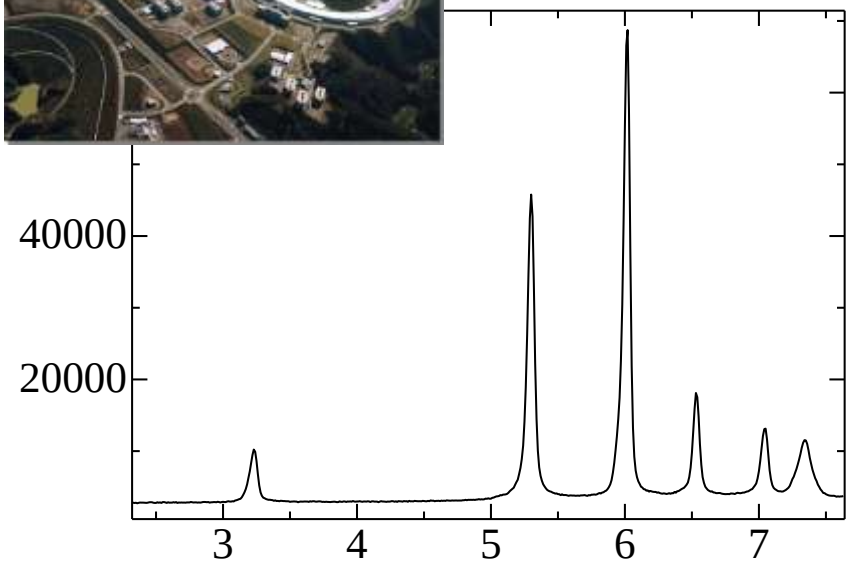

Powder diffraction at SPring-8 has grate advantages in the measurement of small amount of newly synthesized materials.

SR powder diffraction

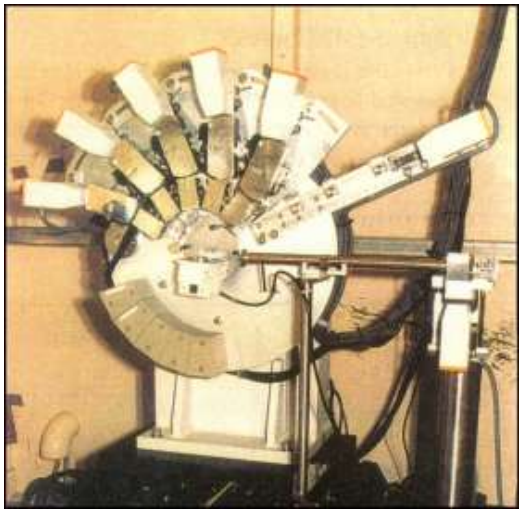

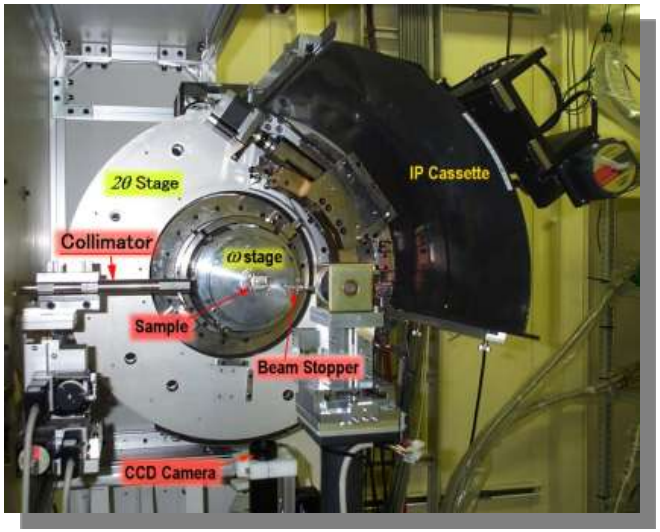

High quality powder diffraction data

- Phase identification
- Qualitative structure analysis,
- Measurements of lattice parameters,
- Estimation of crystallinity, etc.

Quantitative Structure Analysis

- Crystal structure determination
- Crystal structure refinement
- Charge density Study

Structure Analysis of Powder Diffraction Data

Cell Determination

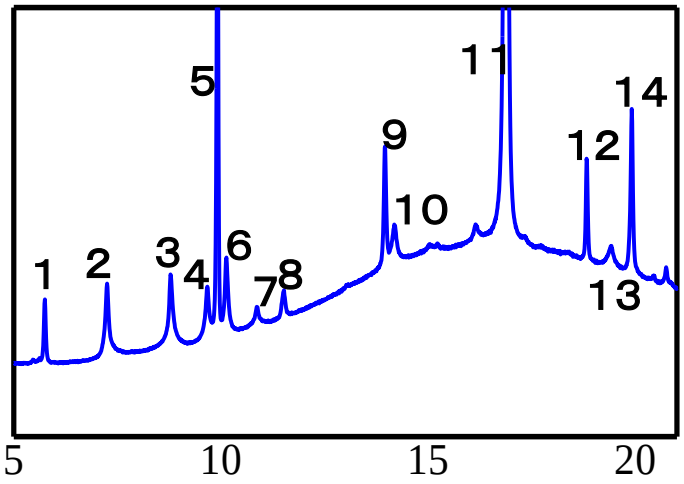

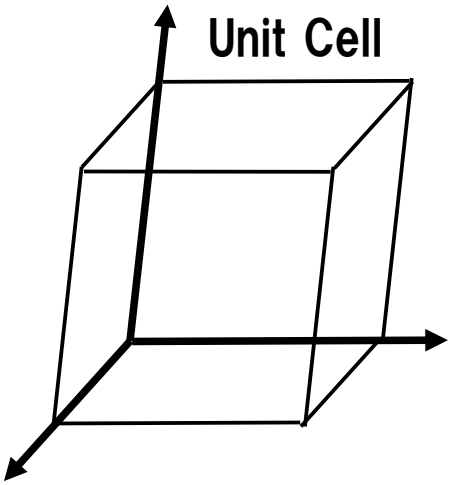

Structure Determination	Direct Method, Direct Space Method
Structural Refinement	Rietveld Method
Accurate Charge Density study	Maximum Entropy Method, Multipole Analysis

Rietveld method

Acta Cryst. 22, (1967) 151-152

Line profiles of neutron powder-diffraction peaks for structure refinement.

H. M. Rietveld,
Reactor Centrum Nederland, Petten, The Netherlands

Received 28 July 1966

H. M. Rietveld

http://home.planet.nl/~rietv025/

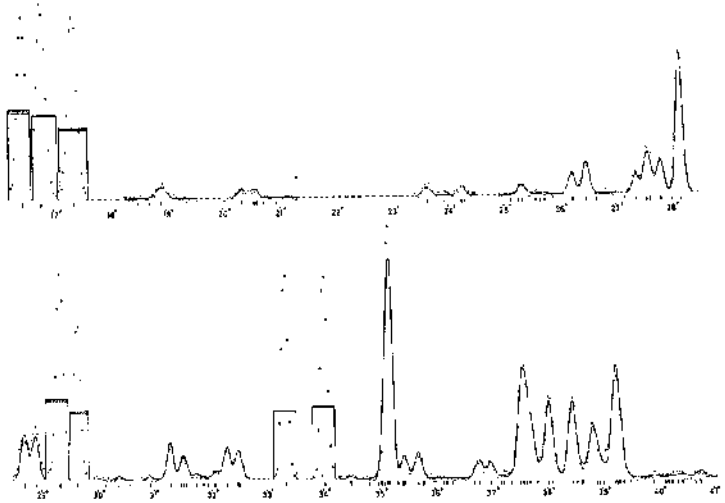

Fig. 1. *Neutron powder diffraction diagram of* WO_3 *(intensity vs* 2θ *). The solid line indicates the calculated profile and the dots the measured intensities. The rectangles represent the integrated single-peak intensities, their different heights the agreement between calculated and observed values.*

Rietveld refinement is a technique devised by Hugo Rietveld for use in the characterization of crystalline materials. The neutron and x-ray diffraction of powder samples results in a pattern characterized by reflections at certain positions. The height, width and position of these reflections can be used to determine many aspects of the materials structure.

Rietveld method

The least-squares refinements are carried out until the best fit is obtained between the entire observed powder diffraction pattern taken as a whole and the entire calculated pattern based on the simultaneously refined models for the crystal structure.

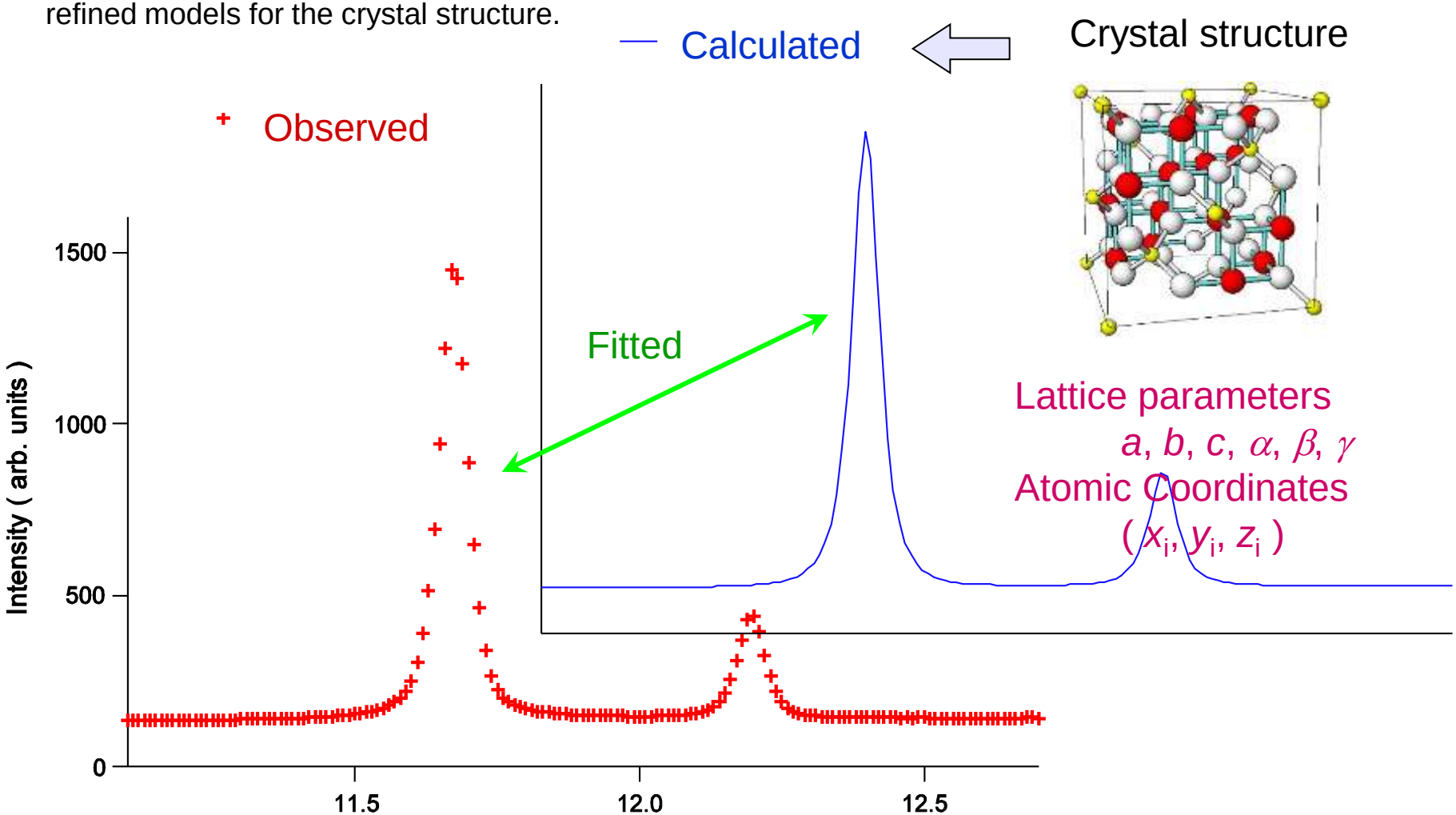

A key feature is the feedback, during refinement, between improving knowledge of the structure and improving allocation of observed intensity to partially overlapping individual Bragg reflections.

Rietveld method

Lattice parameters and atomic coordinates are refined using non-linear least-squares method.

$$\text{Minimize} \qquad S(\boldsymbol{x}) = \sum_i w_i [y_i - f_i(\boldsymbol{x})]^2$$

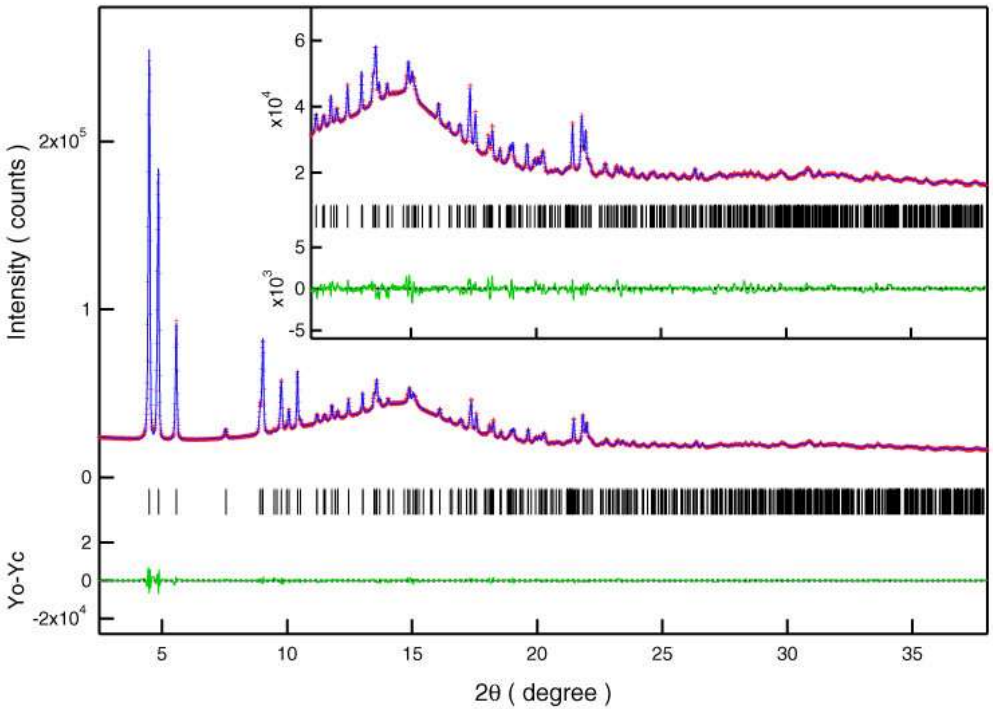

Example of refiend parameters

a=5.1335(2)Å *b*=9.8362(3)Å *c*=10.6881(3)Å

Atom	Site	x	y	z	B(Å^2)
Cu	2a	0.794(1)	0.926(5)	0.518(1)	0.9(1)
O1	2a	0.779(3)	0.912(2)	0.703(1)	0.8(3)
O2	2a	0.139(3)	0.039(1)	0.667(1)	0.8(3)
C1	2a	0.943(3)	0.975(2)	0.741(1)	1.4(2)
C2	2a	0.920(3)	0.964(2)	0.888(1)	1.4(2)
H1	2a	0.752(3)	0.894(2)	0.939(1)	1.4(2)
C3	2a	0.853(3)	0.112(2)	0.907(2)	1.4(2)
H2	2a	0.000(3)	0.182(2)	0.849(2)	1.4(2)

.....

.....

.....

The Rietveld refinement plays an central role of the structure study from powder diffraction.

SR powder diffraction

accurate

Semiconductor

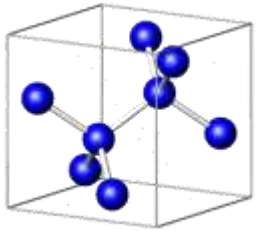

Acta Cryst. A. 2007

Charge density Study

Superconductor

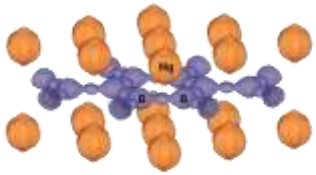

JPSJ. 2001

Ab-initio Strucutre Determination

Thermoelectrics

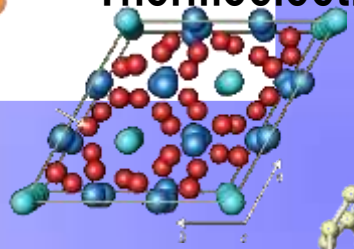

Small

Large

Metal organic materials.

Nano-carbon materiials

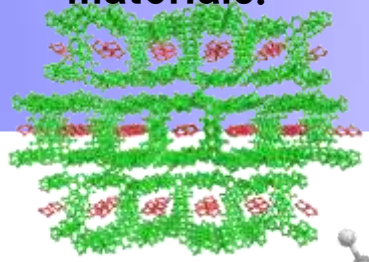

Nature Materials 2004
Phys. Rev. B. 2007

Determination of Disordered Structure

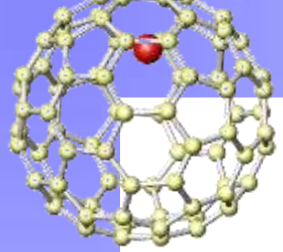

Nature. 2000
Angew. Chem. 2000,2005

Angew. Chem. 2006

Pharmaceuticals

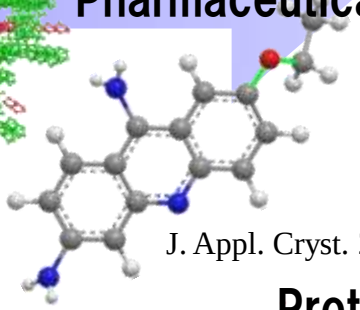

J. Appl. Cryst. 2008

Protein

rough

SR powder structural studies

- Accurate charge density study of silicon and diamond.
- Structural analysis of high performance thermoelectrics Zn_4Sb_3.
- Structure determination of pharmaceutical.

Accurate Structural Study

The electron density distribution in materials determines their properties and functions. Many attempts of both experimental and theoretical researches in materials science have been performed to reveal the electron density distributions.

$$I(\mathbf{k}) \propto \left|F(\mathbf{k})\right|^2 = \left|\int_{UnitCell} \rho(\mathbf{r}) \exp(2\pi i \mathbf{k}\cdot\mathbf{r}) dv\right|^2$$

An X-ray is a very good probe of electrons. The structure factors from X-ray diffraction give information of total electron density distribution including both the core and the valence electrons.

Structure Factors and Charge Density of silicon from SPring-8 Powder Data

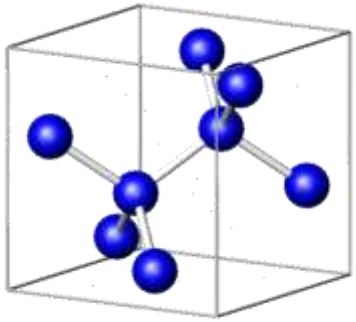

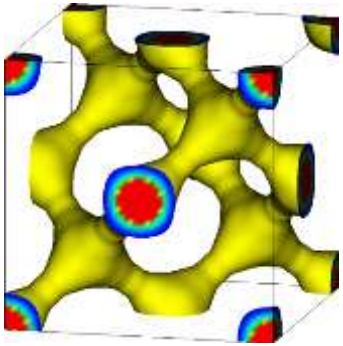

Si

Accuracy of powder data at SPring-8

- Powder data
  dynamic range, resolution
- Structure factors
  compared with other experimental & theoretical data
- Valence charge density
  compared with theoretical data

Powder data of Silicon measured at SPring-8 BL02B2.

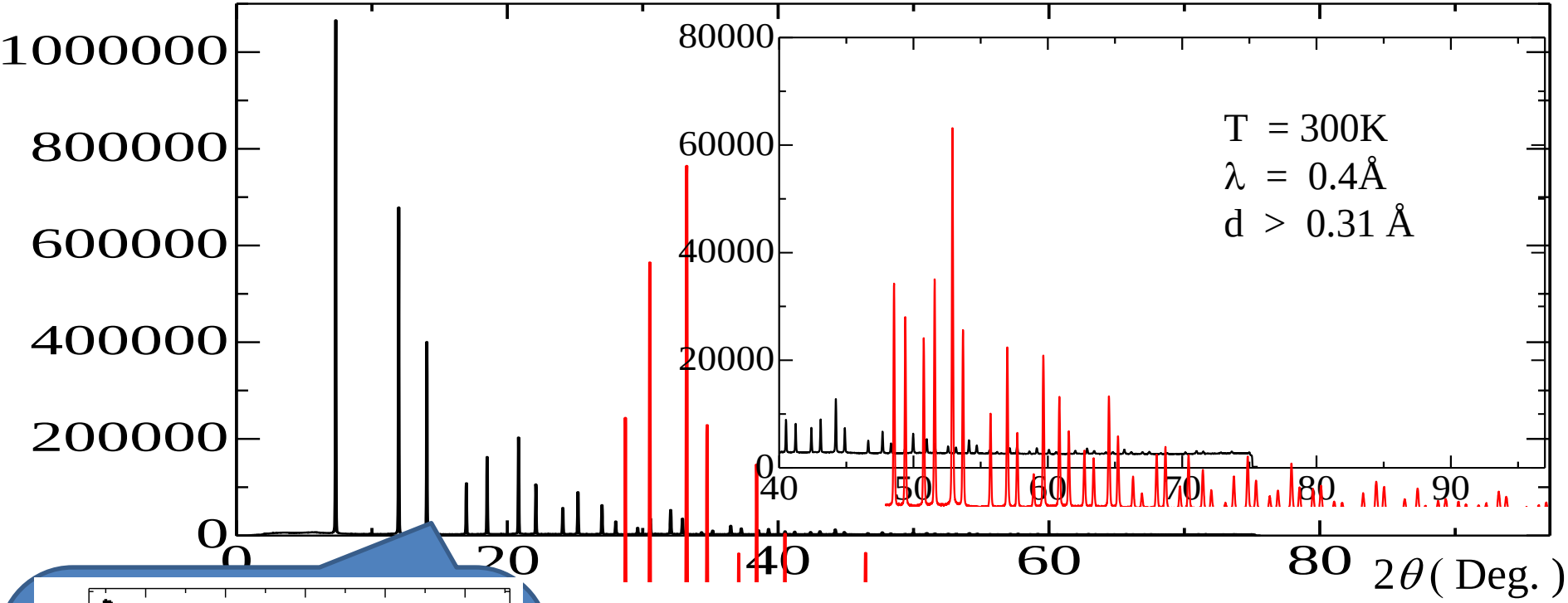

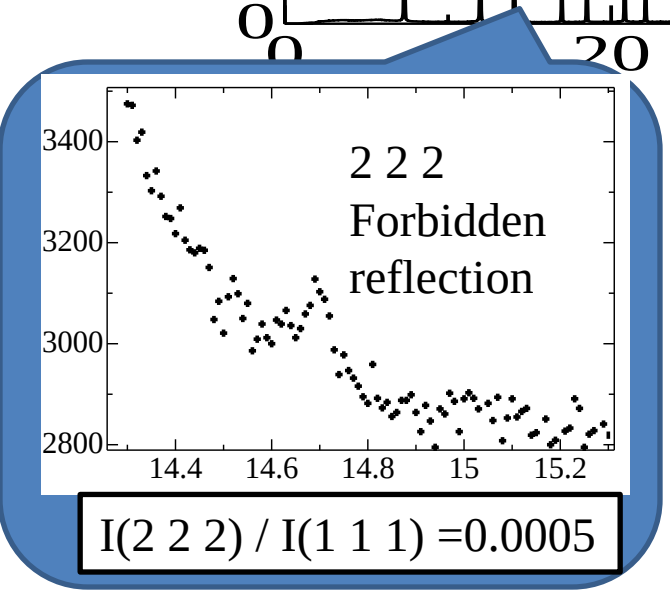

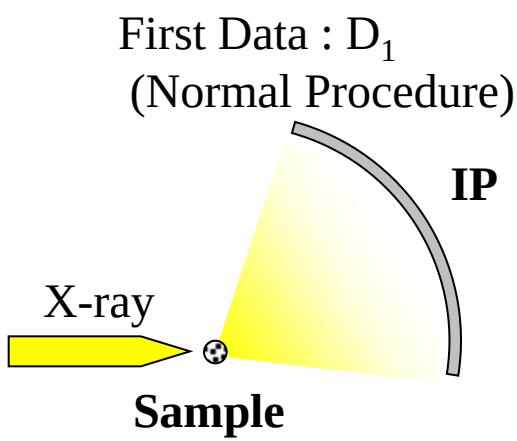

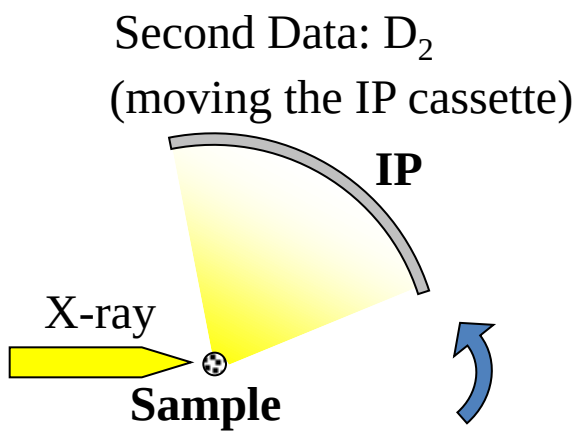

Data Range (2θ)	0～75.0°	40～105.0° (Maximum)

Comparison between Powder data and Saka&Kato's data

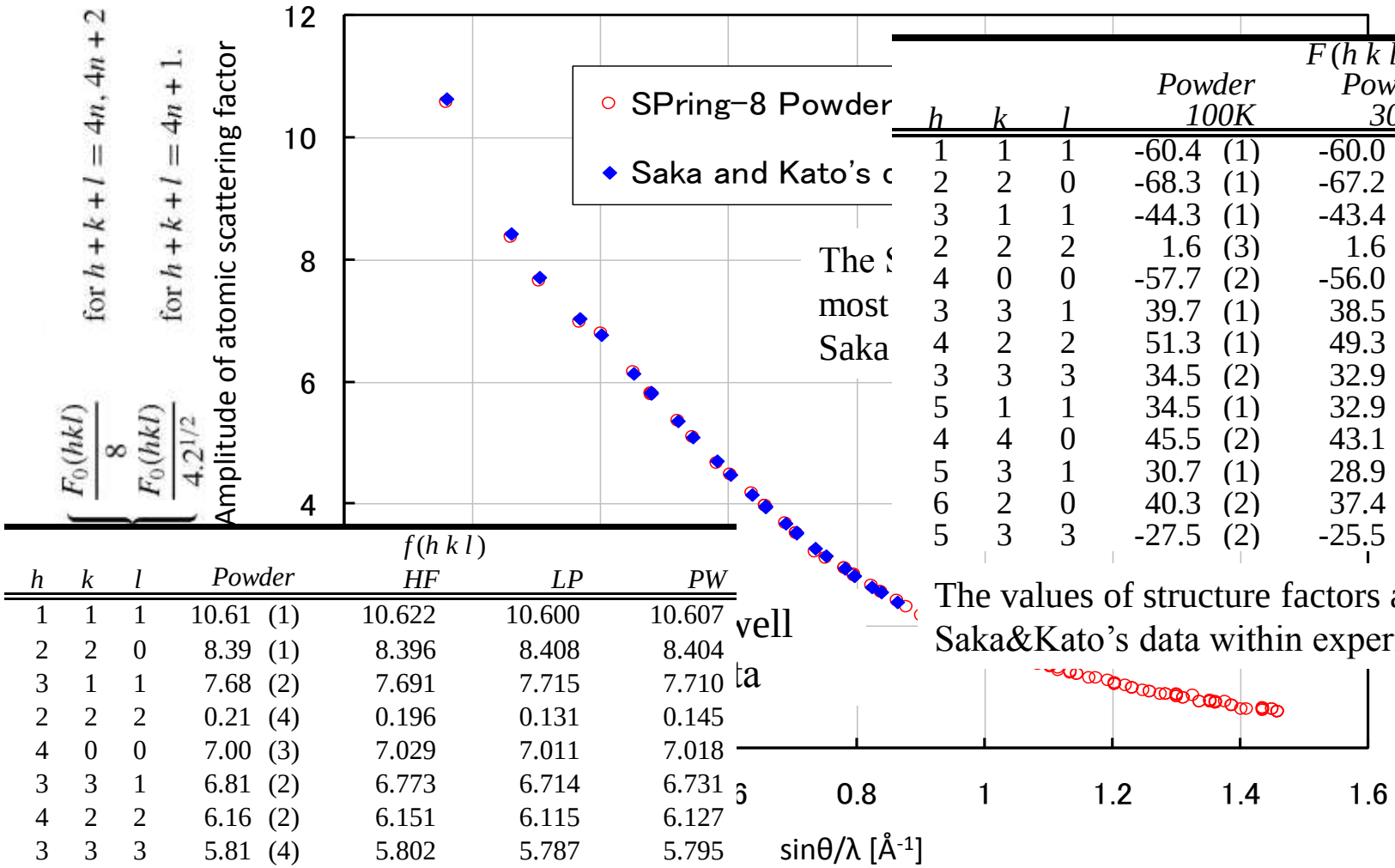

The S
most
Saka
vell
ta

h	k	l	$f(h\,k\,l)$ Powder	HF	LP	PW
1	1	1	10.61 (1)	10.622	10.600	10.607
2	2	0	8.39 (1)	8.396	8.408	8.404
3	1	1	7.68 (2)	7.691	7.715	7.710
2	2	2	0.21 (4)	0.196	0.131	0.145
4	0	0	7.00 (3)	7.029	7.011	7.018
3	3	1	6.81 (2)	6.773	6.714	6.731
4	2	2	6.16 (2)	6.151	6.115	6.127
3	3	3	5.81 (4)	5.802	5.787	5.795
5	1	1	5.82 (2)	5.844	5.810	5.822
4	4	0	5.38 (3)	5.382	5.349	5.360
5	3	1	5.11 (2)	5.110	5.085	5.094
6	2	0	4.68 (2)	4.719	4.696	4.704

h	k	l	$F(h\,k\,l)$ Powder 100K	Powder 300K	Saka Kato 294K
1	1	1	-60.4 (1)	-60.0 (1)	-60.13 (5)
2	2	0	-68.3 (1)	-67.2 (1)	-67.34 (5)
3	1	1	-44.3 (1)	-43.4 (1)	-43.63 (3)
2	2	2	1.6 (3)	1.6 (3)	
4	0	0	-57.7 (2)	-56.0 (2)	-56.23 (4)
3	3	1	39.7 (1)	38.5 (1)	38.22 (3)
4	2	2	51.3 (1)	49.3 (1)	49.11 (4)
3	3	3	34.5 (2)	32.9 (2)	32.83 (2)
5	1	1	34.5 (1)	32.9 (1)	32.94 (2)
4	4	0	45.5 (2)	43.1 (2)	42.88 (3)
5	3	1	30.7 (1)	28.9 (1)	28.81 (2)
6	2	0	40.3 (2)	37.4 (2)	37.59 (6)
5	3	3	-27.5 (2)	-25.5 (2)	-25.36 (4)

The values of structure factors are agreed to Saka&Kato's data within experimental errors

HF: Hartree-Fock, LP:LDA(exchange) and Perdew–Zunger(correlation), PW(GGA): Perdew–Wang(exchangeandcorrelation)

MEM Imaging

Structure Factor for Si by *Pendellösung* Method

T. Saka and N. Kato
Acta. Cryst. **A42**(1986)

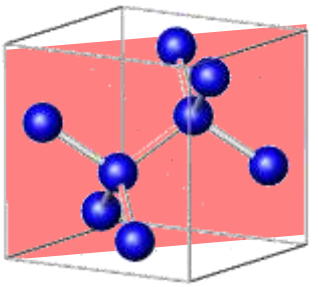

h	k	l	d(Å)	F_{obs}
1	1	1	3.136	60.13(5)
2	2	0	1.920	67.34(5)
3	1	1	1.638	43.63(3)
4	0	0	1.358	56.23(4)
3	3	1	1.246	38.22(3)
4	2	2	1.109	49.11(3)
3	3	3	1.045	32.83(2)
5	1	1	1.045	32.94(2)
4	4	0	0.960	42.88(3)
5	3	1	0.918	28.81(2)
6	2	0	0.859	37.59(6)
5	3	3	0.828	25.36(4)
4	4	4	0.784	33.18(5)
5	5	1	0.761	22.42(3)
7	1	1	0.761	22.37(3)
6	4	2	0.726	29.42(4)
7	3	1	0.707	19.90(3)
5	5	3	0.707	19.98(3)
8	0	0	0.679	26.23(4)
7	3	3	0.664	17.83(3)
6	6	0	0.640	23.48(4)
8	2	2	0.640	23.48(4)
5	5	5	0.627	15.98(2)
7	5	1	0.627	15.98(2)
8	4	0	0.607	21.15(3)
7	5	3	0.596	14.43(2)
9	1	1	0.596	14.46(2)
6	6	4	0.579	19.13(3)

M.Sakata and M.Sato
Acta. Cryst. **A46**(1990)

MEM

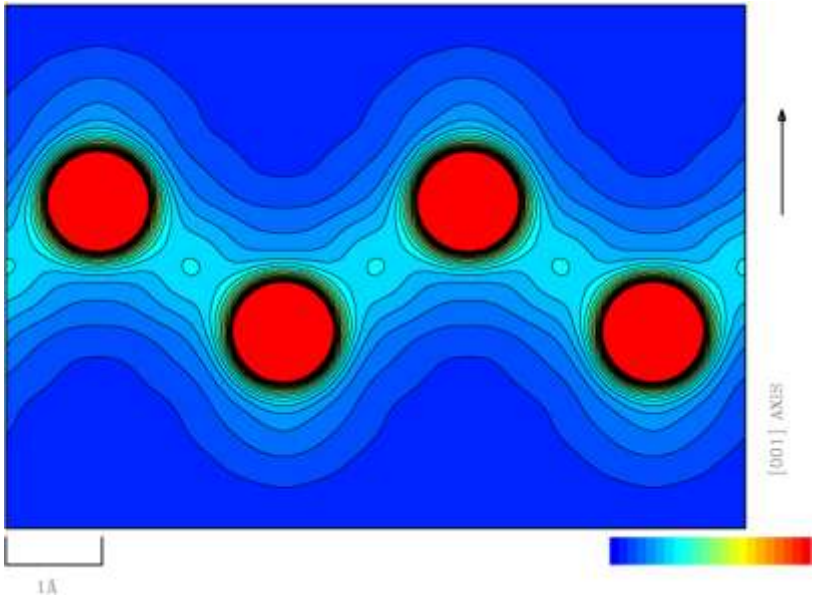

0.1 ～2.0,0.1[e/Å^3] step

The MEM can reconstruct detailed charge density.

MEM for Diffraction Crystallography.

Charge & Nuclear Densities

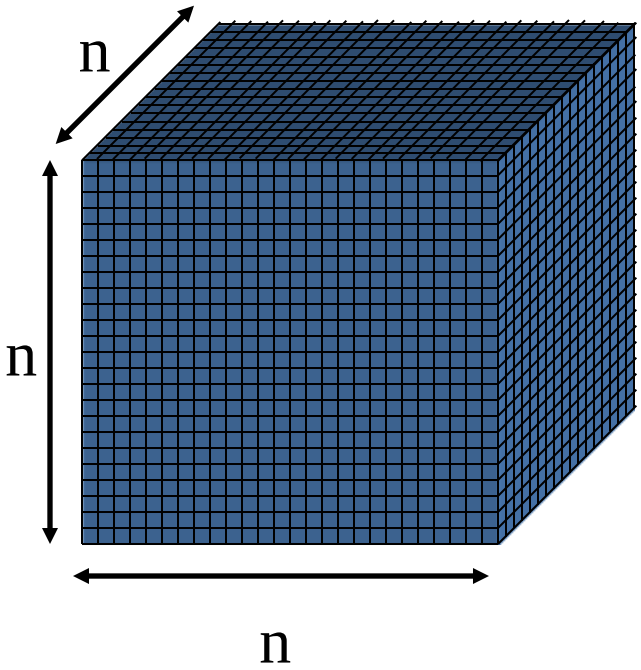

Unit Cell

The unit cell was dividing into the pixels. The density at each pixel is treated as information.

A dimensionless density, ρ'_k, defined as

$$\rho'_k = \rho_k / Q_{tot} \tag{1}$$

Q_{tot} :the total charge in the unit cell.

The entropy for the information of density $S(\rho)$ is defined as

$$S(\rho) = -\sum_{k}^{N_{pix}} \rho'_k \log \rho'_k \tag{2}$$

The MEM searches for the density distribution ρ_k which maximizes the entropy under following condition: $F_{MEM}(h_j)$ agree with $F_{obs}(h_j)$ within σ_j.

$$C(\rho) = \frac{1}{M_{ref}} \sum_{j=1}^{M_{ref}} \frac{1}{\sigma_j^2} |F_{obs}(h_j) - F_{MEM}(h_j)|^2 < 1 \tag{3}$$

$F_{MEM}(h_j)$ calculated from the MEM density are given by

$$F_{MEM}(h_j) = VQ_{tot} \sum_{k=1}^{N_{pix}} \rho'_k \exp(2\pi i h_j r_k) \tag{4}$$

By using Lagrange's method of undetermined coefficients, this problem is reduced to solving simultaneous equations:

$$\rho'_k = \tau_k \exp\left(-\lambda \frac{\partial C}{\partial \rho'_k}\right) \tag{5}$$

τ_k : the prior density. Equations (3), (4) and (5) are solved iteratively.

Valence density based on experimental charge density.

E. Nishibori et al., Acta. Cryst. A (2007)

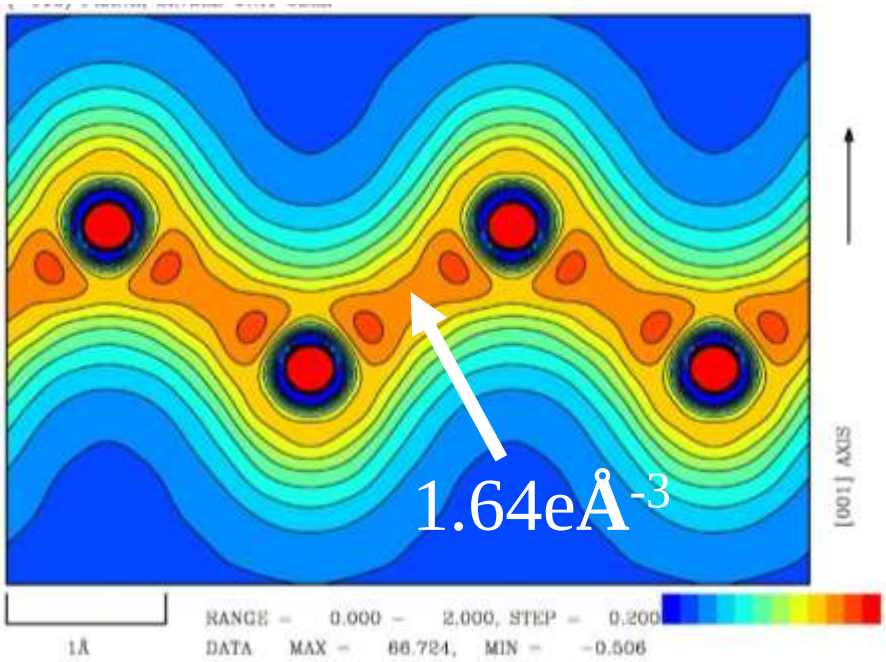

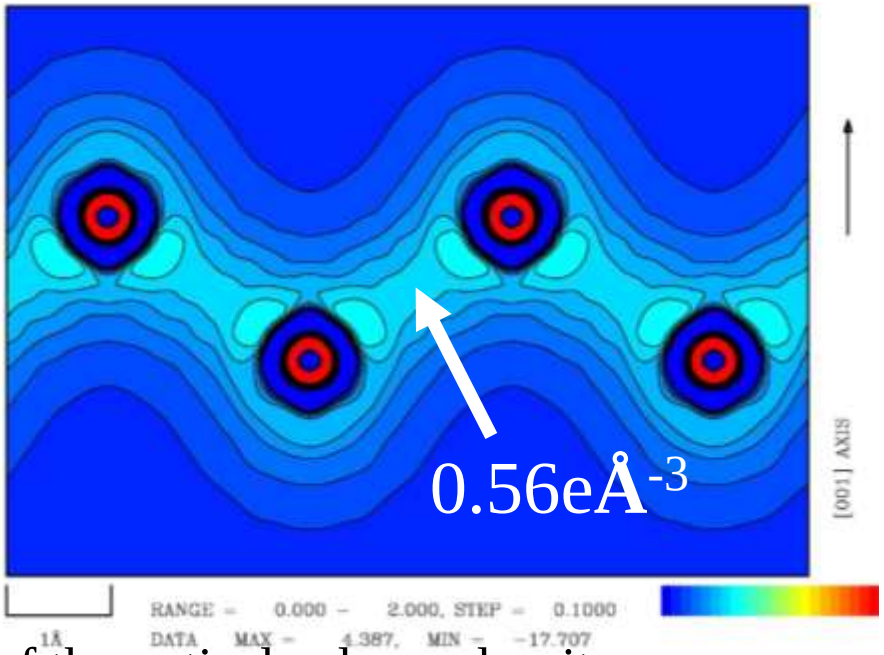

Charge Density at Bond mid-point of theoretical valence density

Si : 0.55～0.59eÅ^{-3}

Diamond :1.53～1.69eÅ^{-3}

Yin M. T. And Cohen M. L., PRB26 (1982). Van Camp P. E., et al., PRB34,(1986)., Christensen N. E. et al., PRB36 (1987). , etc.

The facts can be regarded that the charge densities from SPring-8 powder data are quantitative reliable and can be used to discuss the physical properties of materials.

High performance thermoelectrics Zn_4Sb_3

a Cailat et al, J. Chem. Phys. Solid.(1997)

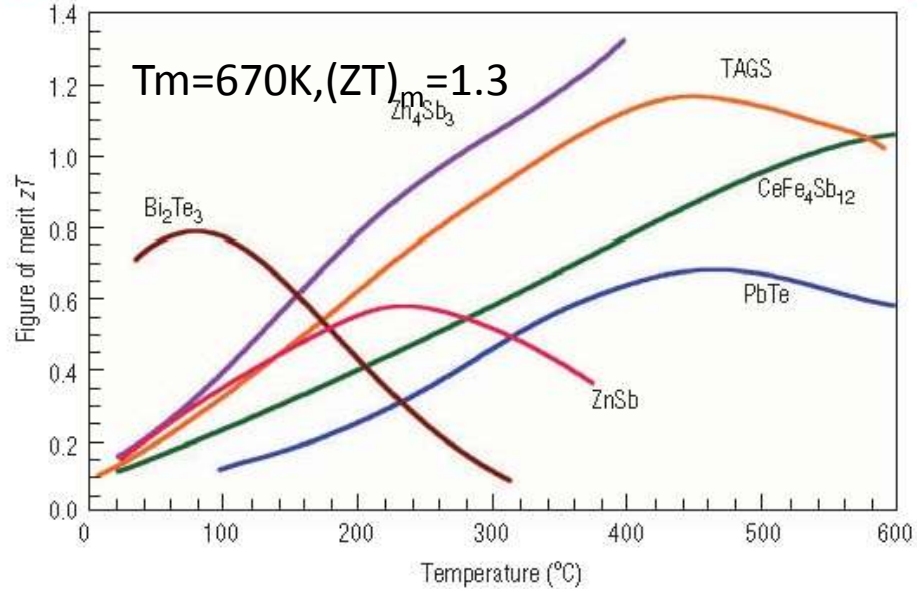

b

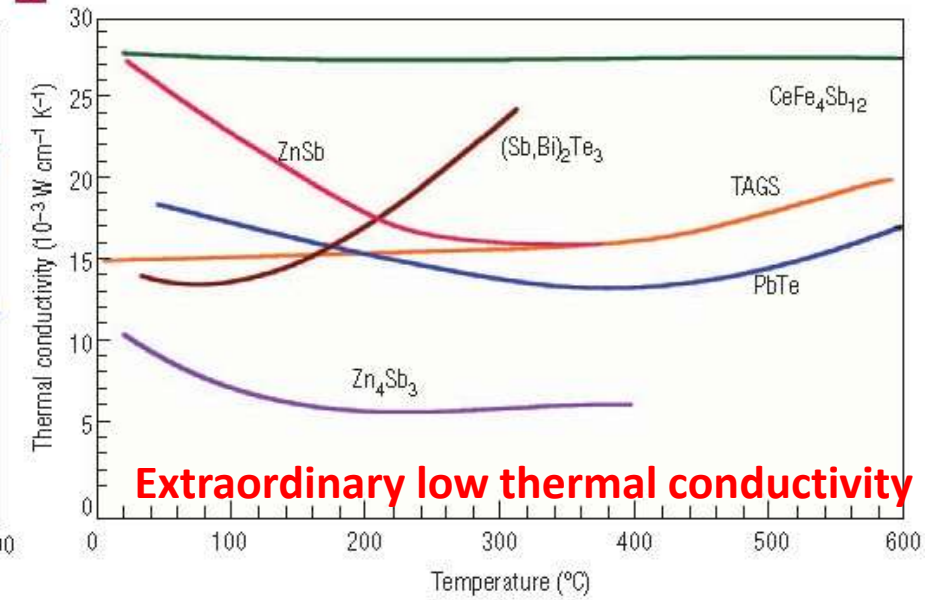

$$ZT = \frac{TS^2\sigma}{\kappa}$$

σ : Electrical conductivity
κ : Thermal conductivity
S : Seebeck coefficient
T : Temperature

Structure of Zn_4Sb_3 by H. W. Mayer et al(1978)

site		
Sb1	18e	Sb(89%)/Zn(11%)
Sb2	12c	Sb(100%)
Zn	36f	Zn(100%)

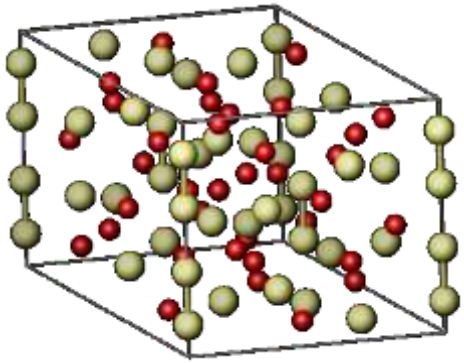

Density 6.21(g cm^{-3})
Zn_xSb_3 x=4.07

Density of *ZT*=1.3 sample by immersion method:6.36(g cm^{-3})

Structural study of Zn_4Sb_3 Thermoelectric

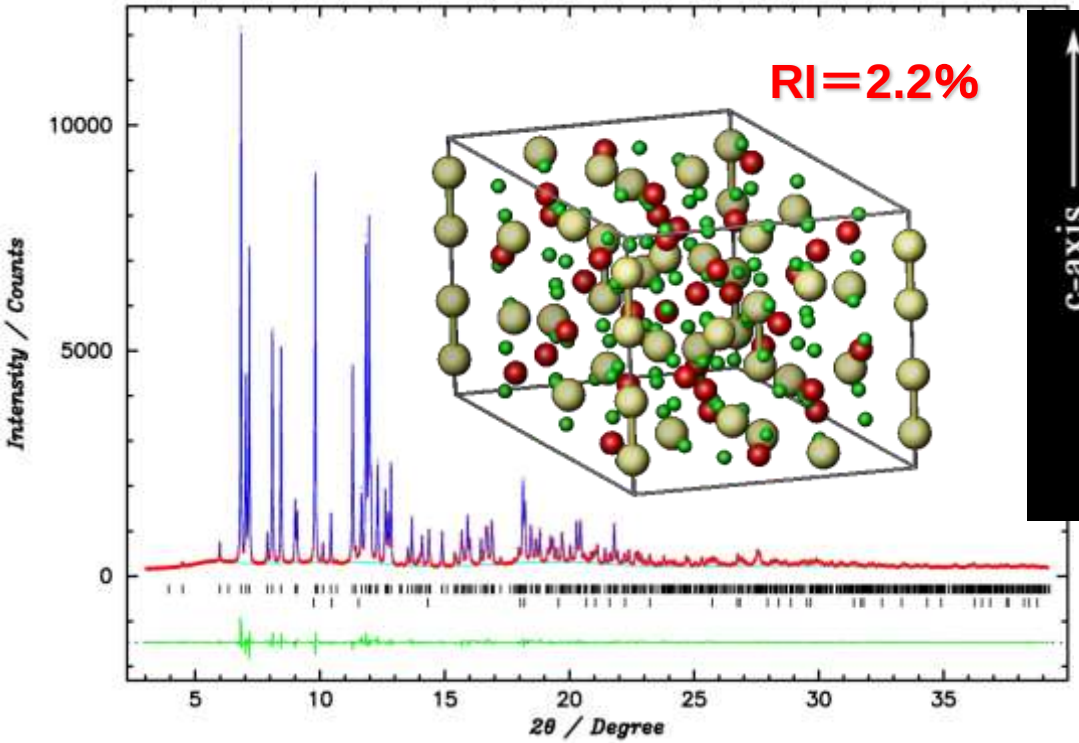

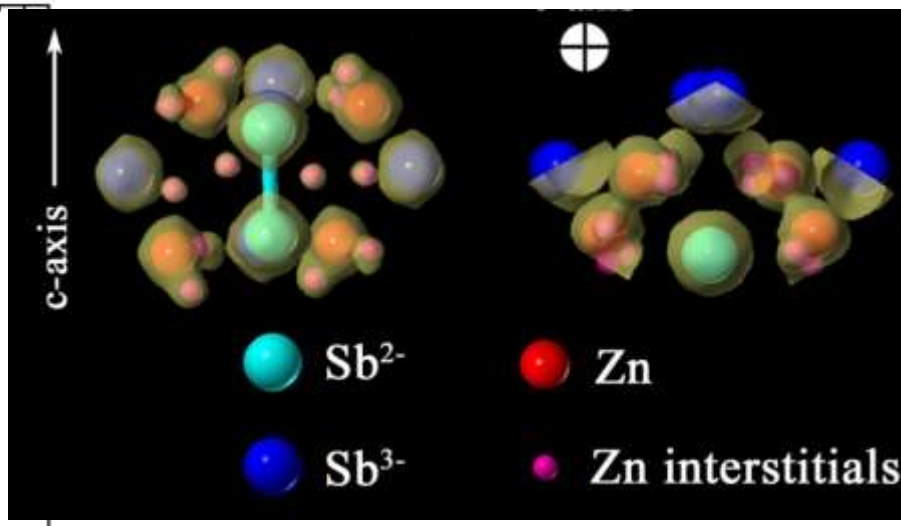

Disorder Structure of Zn

The structure determined in the present study reveals disordered interstitials as an effective mechanism for low thermal conductivity that makes Zn_4Sb_3 the highest *zT* thermoelectric in the 150–400℃ temperature range.

Nature Materials.(2004)
Chemistry - A European Journal (2004).

Density(gcm^{-3})			**6.37**		
Atom	Site	X/a	Y/b	Z/c	Occupancy
Zn(A)	36f	0.07915(4)	0.24483(6)	0.40273(5)	0.899(1)
Zn(B)	36f	0.1782(8)	0.434(1)	0.030(1)	**0.068(1)**
Zn(C)	36f	0.2391(7)	0.4553(8)	0.2093(3)	**0.068(1)**
Zn(D)	36f	0.131(1)	0.233(1)	0.278(1)	**0.033(1)**
Sb(1)	18e	0.35559(3)	0	0.25	1.0
Sb(2)	12c	0	0	0.13646(2)	1.0

Structure Determination from Powder Diffraction data. (SDPD)

SDPD has attracted wide interests for its huge potential to accelerate a design, synthesis, and characterization of the materials in the fields of materials science.
The most important progresse of SDPD is the development of the **direct-space method**.

Direct Space Method

The structure is defined by a rigid body of molecule.

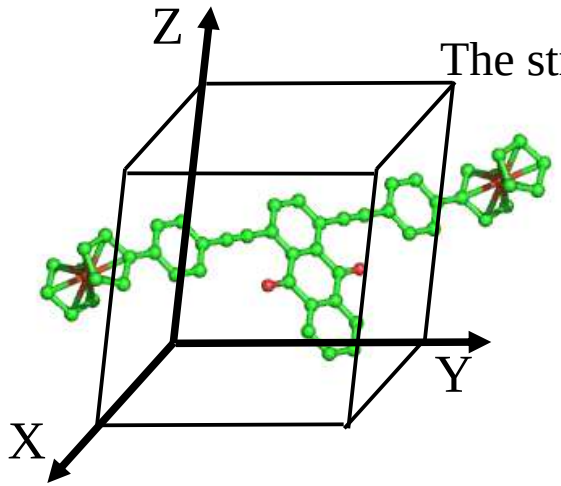

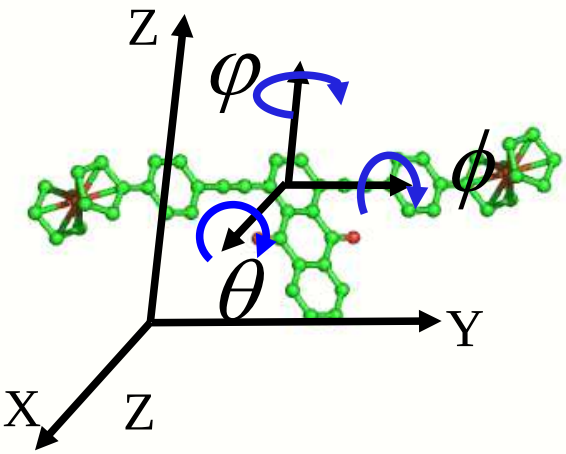

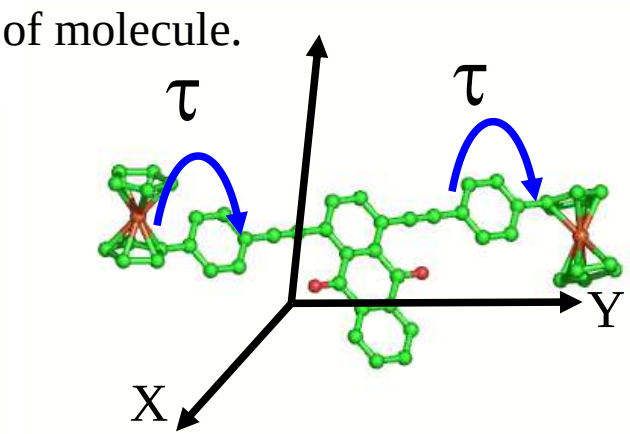

If the molecular conformation is not known, it is necessary to include a number of torsion angles as parameters.

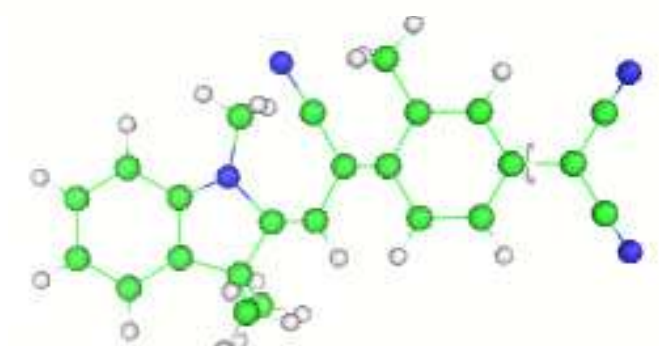

Torsion Angle(τ)

Trial structures are randomly generated in real space at first.

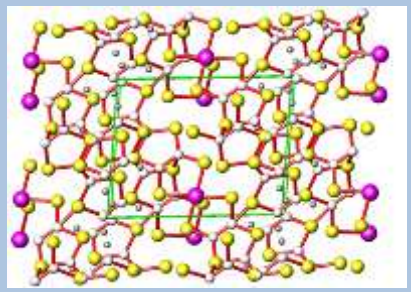

$\Gamma[x1, y1, z1, \theta1, \phi1, \psi1]$

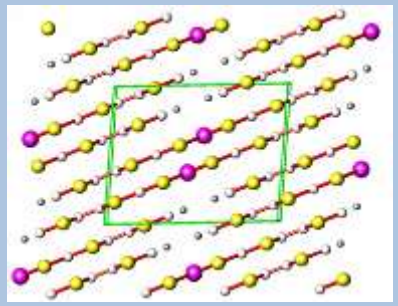

$\Gamma[x2, y2, z2, \theta2, \phi2, \psi2]$

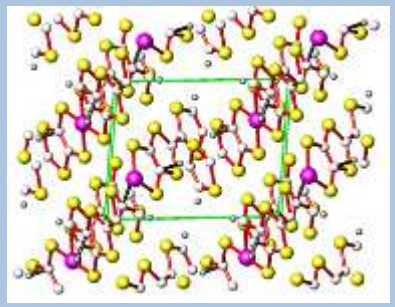

$\Gamma[x3, y3, z3, \theta3, \phi3, \psi3]$

Calculate powder data

Comparison between observed and calculated data

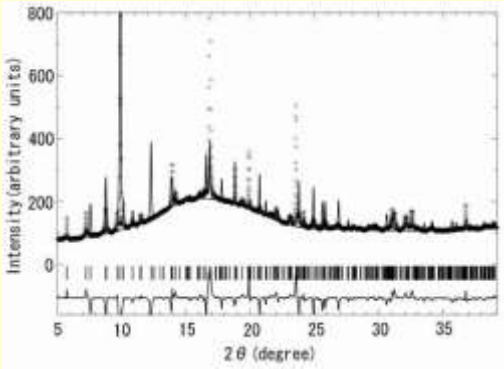

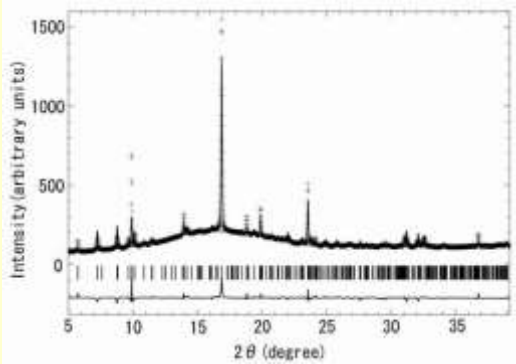

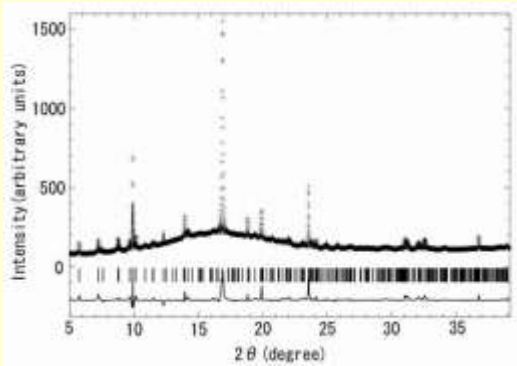

Optimization methods.

- Monte Carlo
- Simulated Annealing
- **Genetic Algorithm**

GA for SDPD

(K. D. M. Harris et. al.,)

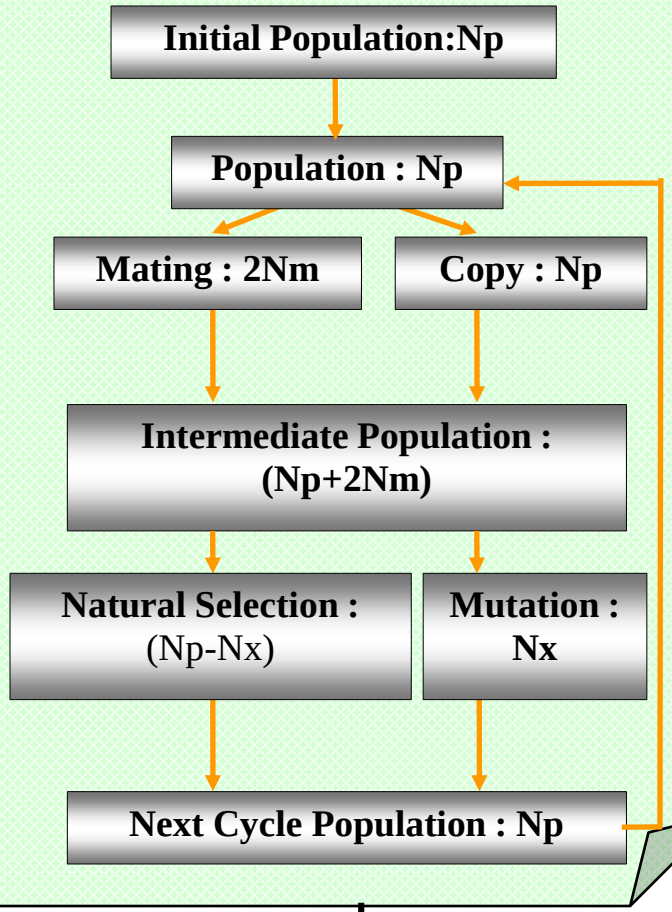

+

Blend cross over(BLX-α)
Minimum generation gap(MGG)
Partial minimization etc.

M. Sakata and E. Nishibori, JP2005－350770,
M. Sakata and E. Nishibori, PCT/JP2006/324614

SDPD for large systems with more than 100 atoms and 20 degrees of freedom(DOF) is very difficult.

Prednisolone Succinate, $C_{25}H_{32}O_8$

Space Group *I*2,
Cell Volume 4622.4(2) $Å^3$

Number of molecule in asymmetric unit = 2

Number of atoms[65×2]=130

Number of Torsion angle = 7

DOF[(6+7)×2-1]=25

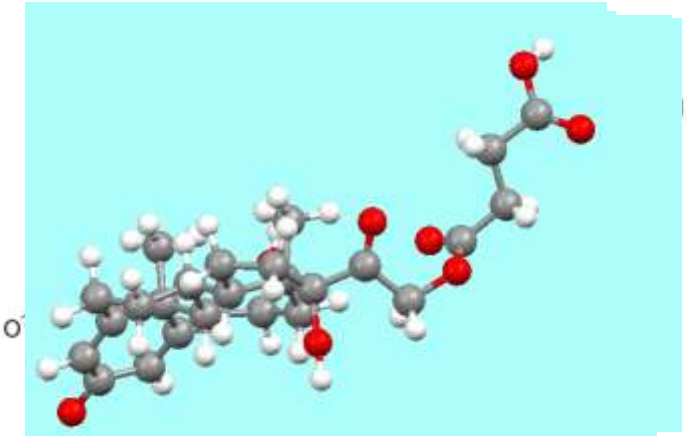

The largest target for SDPD.

Final result of Refinements

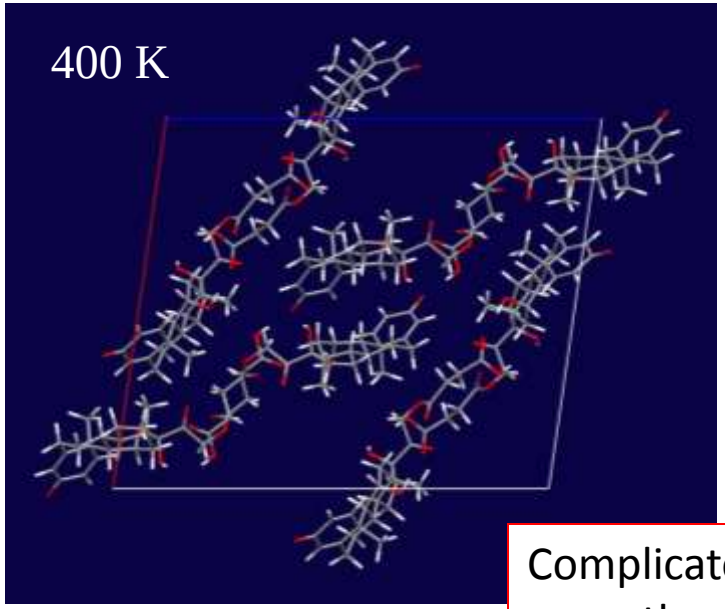

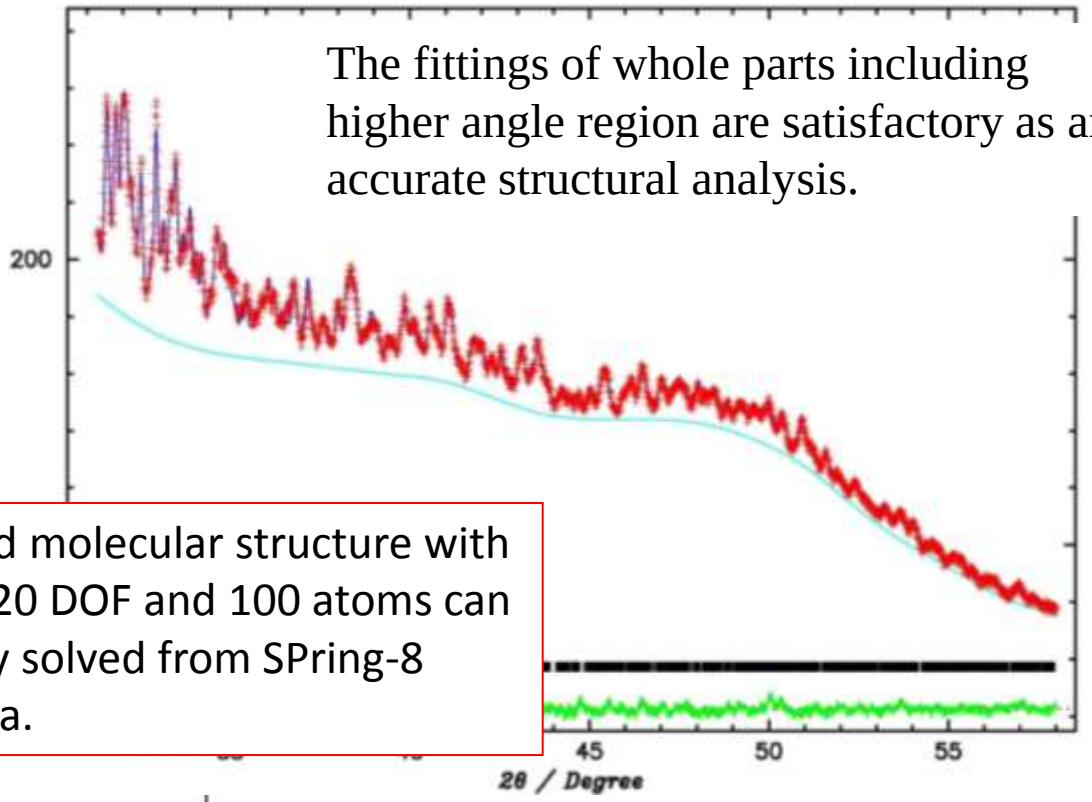

The fittings of whole parts including higher angle region are satisfactory as an accurate structural analysis.

Complicated molecular structure with more than 20 DOF and 100 atoms can be routinely solved from SPring-8 powder data.

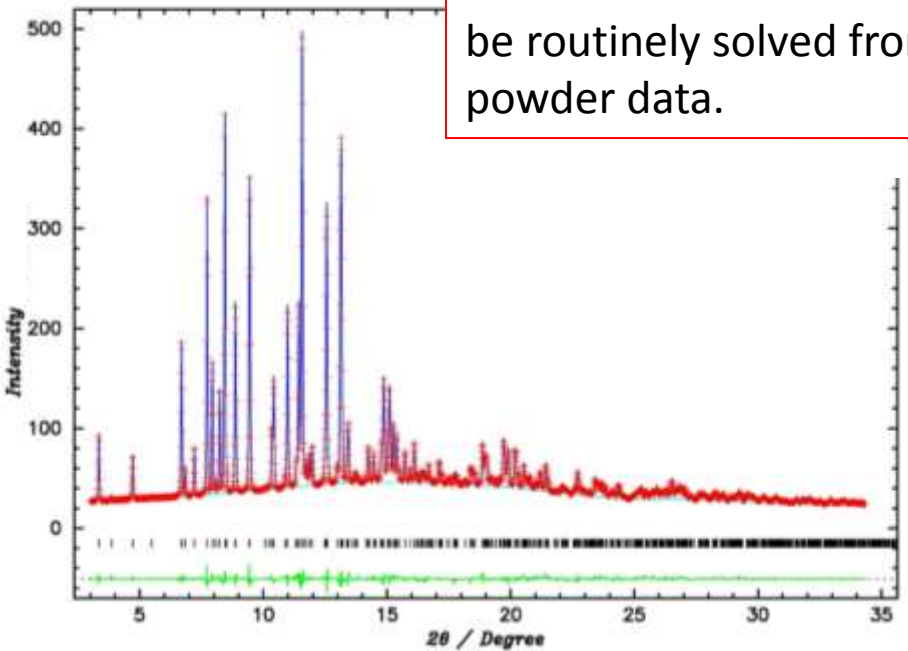

R_{WP}= 1.29 %

R_I= 4.80 %

d > 1.03 Å

There were no unreasonable bond distances and bond angles in the refined structure.

J. Appl. Cryst. (2008)

Summary

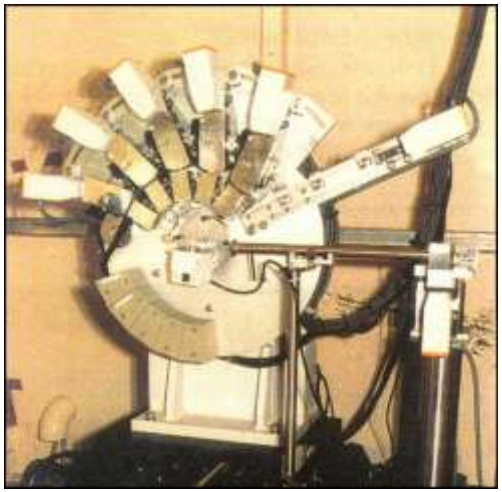

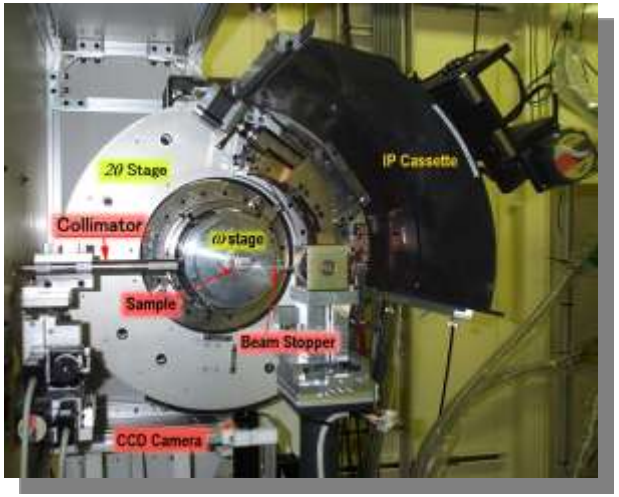

Materials Science

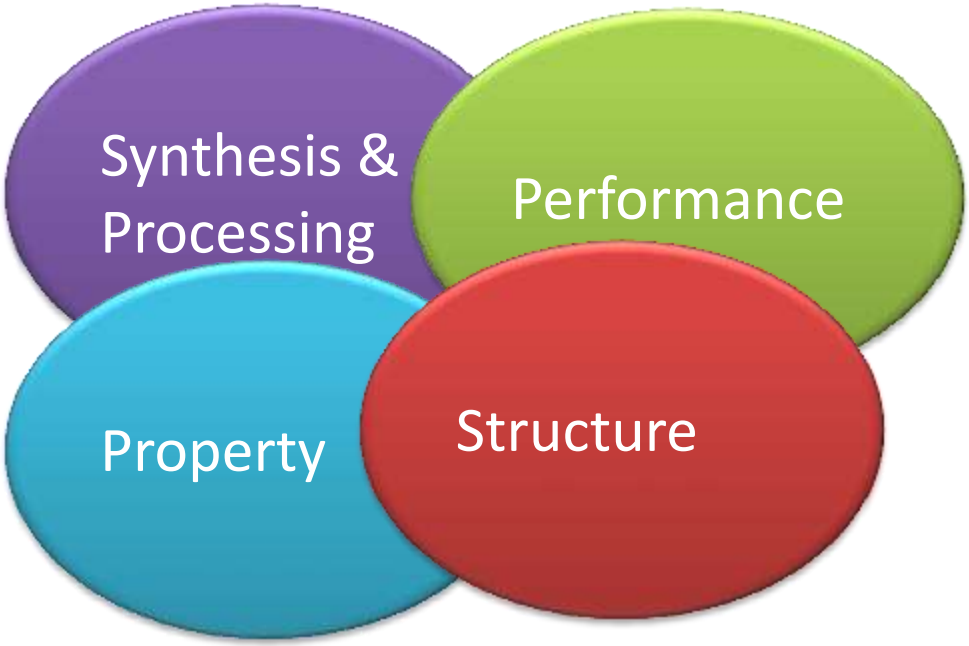

The structural changes induced by an external field

- Temperature
- Light
- Gas/and Solvent absorption

SR Powder structural study now covers wide area of materials science.